Postprint of: Czechowska J., Kawecka A., Romanowska A., Marczak M., Wityk P., Krzymiński K., Zadykowicz B., Chemiluminogenic acridinium salts: A comparison study. Detection of intermediate entities appearing upon light generation, Journal of Luminescence, Vol. 187, (2017), pp. 102-112, DOI: 10.1016/j.jlumin.2017.02.068

Chemiluminogenic acridinim salts: a comparison study. Detection of intermediate entities appearing upon light generation

Justyna Czechowska, Alicja Kawecka, Anna Romanowska, Maria Marczak, Paweł Wityk, Karol Krzymiński* and Beata Zadykowicz*

Faculty of Chemistry, University of Gdańsk, Wita Stwosza 63, 80–308 Gdańsk, Poland

Abstract

The nine derivatives of acridine-9-carboxylic acid (CMADs) capable for chemiluminescence (CL), representing various classes of compounds were isolated in a chemically pure state (assessed by RP-HPLC) and identified using high resolution mass spectrometry (ESI-QTOF) and magnetic resonance (^{1}H NMR) techniques. Among them are aryl acridinium esters, containing certainly selected and located substituents in both aromatic systems, an acridinium perfluorinated aliphatic ester and an acridinium sulfonamide. The main aim of the study was to compare, under the conditions of their optimal performance, the luminogenic properties of the above molecular systems, such as efficiency and kinetics of emission, limits of detection/quantification as well as stability in aqueous solutions. All of the investigated acridinium salts can serve as CL indicators or fragments of CL labels in modern medical diagnostics (e.g. chemiluminescence and electrochemiluminescence immunoassays (CLIA, ECLIA), hybridization protection assays of nucleic acids (HPA) as well as other ultra-sensitive luminescence tests. Taking advantage of the flow injection mass analysis, the appearance of unstable cationic intermediates produced upon chemiluminogenic oxidation of selected acridinium salts in an alkaline environment was confirmed for the first time. The observed entities include hydroxyl and hydroperoxide adducts (as radical cations) as well as the acridan spirodioxetanone derivative, making a high energetic and direct precursor of the target emitters, an electronically excited 10-methylacridan-9-ones. The results are supported with quantum chemistry calculations at the DFT level of theory. Theoretical studies have helped to determine the unstable intermediates appearing during in CL in ESI-QTOF experiments. In the group of acridinium ester they allowed to observe the positive linear trend

*Correspondence to: Faculty of Chemistry, University of Gdansk, Wita Stwosza 63, 80–308 Gdansk, Poland.
E-mail: karol.krzyminski@ug.edu.pl (K. Krzymiński), beata.zadykowicz@ug.edu.pl (B. Zadykowicz).

among between the kinetics of CL decay and calculated coefficients of p_z LUMO orbitals on the carbon atoms being the reaction centers responsible for generation of light.

Keywords

Chemiluminescence; Acridinium salts; ESI-QTOF MS spectrometry; Reaction intermediates; Spirodioxetanone; Surfactants; DFT methods; Enthalpy and Gibbs free energy

Introduction

About 50 years ago researchers turned their attention to the promising chemiluminogenic systems based on 10-substituted acridine-9-carboxylic acid derivatives, containing 9-cyanoacridinium [1,2], 9-[phenoxy(carbonyl)]acridnium [3–8] and 9-[(sulfonyl(amido)]acridinium cations [9,10], prone for the nucleophilic addition (CMADs). These derivatives may undergo oxidation by H_2O_2 or other oxidants in alkaline media, yielding electronically excited 10-methyl-9-acridinones, that are able to emit light in visible range of spectrum [11,12]. The phenomenon, known as chemiluminescence (CL), has been the subject of thorough investigations and has found numerous applications in clinical [12,13], pharmaceutical [14], chemical and biochemical [15–17] as well as in environmental [18] and food analysis [19,20]. The 10-substituted acridinium cations mentioned above have been the subject of many investigations, both of a cognitive [1,2,4,6,9,10] and utilitarian [12,13,18,21–23] nature. The reason for this was that they can serve as CL indicators or fragments of labels in extremely sensitive quantitative determinations (limits of detection at the level of 10^{-19} mole of analyte or below) of a wide range of entities of biological importance such as antigens, antibodies, nucleic acids, hormones, food additives hydrogen peroxide and others [12–20].

Taking into account the chemiluminogenic properties of acridinium salts and their practical importance, an understanding of the processes giving rise to the emission of light seems to be indispensable. The mechanism of chemiluminogenic oxidation of some of 10-alkylated acridinium cations with hydrogen peroxide in alkaline media has been discussed by several authors [4,7,11,24] and examined in our group in detail for the acridinium esters (AE) at the semiempirical (PM3-COSMO) [4] and density functional levels of theory [7,8]. The mechanism of the mentioned multi-staged process is thought to proceed by the initial attack of the hydroxyperoxide anion at the carbon atom in position 9 of the acridinium nucleus, following by an immediate reaction of such formed adduct with hydroxide anion

(essentially with no kinetic barrier) to form a cyclic intermediate (the peroxy-type of ion) or – after elimination of respective aryloxy anion – a highly energetic acridan spirodioxetanone cyclic intermediate [7,8,25]. The above entities may spontaneously decompose with the generation of electronically excited molecules of 10-methyl-9-acridinones and aryl carbonate anions or carbon dioxide – depending on subtle differences in the structure of the chemiluminogenic substrate [4]. However, in an alkaline environment and in the absence of hydrogen peroxide, AEs hydrolyze more or less rapidly with the formation of 10-methylacridinium-9-carboxylate anions; simultaneously with the alkaline hydrolysis some other dark processes occur, indicated by the formation of the so-called 'pseudo-base' of the acridine carboxylic acid derivative [8] and finally – 10-methyl-9-acridinone in the ground electronic state. According to the quantum chemistry calculations, the thermodynamic data obtained theoretically is, in general, well comparable to the experimental findings [25]. Chromatographic (RP-HPLC) analyses of post-CL reaction mixtures revealed that adequate 10-methyl-9-acridinone, phenol and 10-methylacridinium-9-carboxylic acid derivatives make the final products after CL completion of AEs [25]. However, the above mentioned chromatographic and other standard approaches (electronic spectroscopy – UV-Vis and fluorescence emission) revealed only stable products of reaction, but did not shed light on the intermediate forms (chemically unstable and short-living) and thus only in a fragmentary way explained the mechanism of chemical transformations of the light-generating acridinium salts. An efficient transformation of acridinium salts to the cyclic forms and then – to the electronically excited molecules, as well as a limitation of the dark processes (hydrolysis and non-CL reactions) are important issues for the rational design of new acridine-based chemiluminogens of potential utility. These are related to the structure of chemiluminogenic compounds, the features of the environment and the type of triggering reagents used for the initiation of CL. The former investigations revealed, that the chemiluminogenic properties of AEs are controlled by the acidity (pK_a) of the leaving groups, the volume of their hydration layer resulting from the substitution in the benzene and/or acridinium moieties, altering the electronic properties of the aromatic ring systems [7]. As regards other factors, it was well proved that selected surfactants (at certain concentrations) may substantially enhance the emission efficiency and dramatically alter the reaction kinetics in the aqueous phase. Taking into account the triggering reagents, hydrogen peroxide seems to be the best oxidizer when applied at low concentrations (optimally in the range of 2–4 mM); organic peroxides such as *tert*-butyl hydroperoxide or lauroyl peroxide, do not initiate the efficient emission of light [7].

Among bases tested in the context of AE chemiluminescence, the optimal choice seems to be tetra-n-butylammonium hydroxide besides of typical reagents employed for that purpose such as sodium or potassium hydroxide (NaOH or KOH).

Our recent investigations on the CL of acridinium salts were targeted on the systematically substituted families of aryl esters of 10-methylacridinium-9-carboxylic acids, containing atoms or groups of various electronic or steric character (alkyl, halogens, nitro, methoxy and trifluoromethyl) attached at *ortho*-, *meta*- or *para*-positions of the benzene ring [8]. Natrajan et al. performed thorough studies on the family of acridinium ester-based CL labels and their protein conjugates and they determined some structural and environmental features of such systems influencing the emission properties of such compounds. According to them, 2-alkoxy-substitution in the acridinium ring system and the introduction of zwitterionic fragments (involved in substituents or surfactants) seem to be beneficial from the point of view of CL efficiency [6].

In the presented work we have focused on the investigation of how the properties of the leaving group and the substituent in the acridinium moiety affect the chemiluminogenic properties of respective quaternary derivatives. According to this, nine derivatives of 9-carboxy-10-methylacridinium acid (CMADs, indicated in Table 1), containing in both aromatic systems various chemical functions of different electron-donor-acceptor and steric properties (substituted aromatic ester, highly fluorinated aliphatic ester, sulfonamide group, fluorine atom), were synthesized and characterized in terms of their structure and physicochemistry. The compounds were selected on the basis of extensive research on the chemiluminogenic acridinium salts undertaken up to date [7,8,10]. We have compared the effect of derivatization of the carboxylic group and the acridinium moiety as well as the influence of environment (base, additives) on the chemiluminogenic properties (efficiency of emission, kinetics of CL decay) of respective CMADs.

Applying the ESI-QTOF mass spectrometry, supported by the quantum chemistry calculations, some of the crucial intermediate products of the oxidation of CMADs with hydrogen peroxide in alkaline media (involved in the generation of CL) have been identified. Density functional theory (DFT) computations have been employed for comparative study to better understand the processes giving rise to the emission of light and to support the interpretation of the results obtained experimentally.

Experimental

Synthesis and identity of compounds

9-Carboxy-10-methylacridinium derivatives (CMADs, Table 1) were synthesized by optimizing known methodologies, as it is reported in SI [7,8,26]. All chemicals were purchased from Sigma-Aldrich, unless indicated otherwise. Compounds **1**–**9** were subjected to melting point determination (Melting Point M-565, Büchi, Switzerland). Their purity was assessed through application of the reversed-phase high-performance liquid chromatography (RP-HPLC) method (Waters 600 E Multisolvent Delivery System, Waters 2487 Dual λ Absorbance Detector; stationary phase: Gemini 5μ C6-Phenyl 110A, 100×4.6 mm column (Phenomenex); isocratic mobile phase: 1 ml/min, acetonitrile/0.1% trifluoroacetic acid in UP water (1/1 v/v); absorbance detection at 254 and 365 nm). The identity of acridinium cations involved in **1**–**9** was confirmed by ESI-QTOF spectrometry (TripleTOF™ 5600$^+$, AB SCIEX, Canada) and ^{1}H NMR spectra, recorded at r.t., employing Advance III 500 MHz spectrometer (Bruker, USA).

The analyses of compounds **1**–**9** are listed below in the following manner: retention factor related to uracil (k), assessed by RP-HPLC; melting point (m.p.); molecular ion (M^+ in m/z); ^{1}H NMR signals (solvent): chemical shift (δ) in ppm (integration, multiplicity, conjugation constant (J) in Hz). For **1**: k = 1.69, m.p. = 534.6 K, M^+ = 376.11; ^{1}H (DMSO-d6): 8.95 (2H, d, 9.3), 8.63 (2H, d, 8.1), 8.57 (2H, t, 8.8), 8.19 (2H, t, 8.4), 7.64 (2H, s), 4.96 (3H, s), 2.08 (6H, s). For **2**: k = 0.80; m.p. = 501.6 K; M^+ = 387.13; ^{1}H (CD_3CN): 8.75 and 8.68 (2H, d, 8.5), 8.59 and 8.48 (2H, d, 8.8), 8.55 (2H, t, 5.0), 8.29 and 8.03 (2H, t, 5.0), 8.22–8.17 (2H, m), 4.96 (3H, s), 2.59 (6H, s). For **3**: k = 1.74, m.p. = 514.8 K, M^+ = 390.14; ^{1}H (DMSO-d6): 9.02 (2H, d, 9.4), 8.74 (2H, d, 7.9), 8.63 (2H, t, 8.7), 8.26 (2H, t, 8.3), 7.98 (2H, d, 11.2), 7.93 (2H, d, 11.2), 7.82 (2H, d, 7.1), 7.60 (2H, t, 7.7), 7.50 (1H, t, 7.6), 5.03 (3H, s). For **4**: k = 1.06; m.p. = 531.6 K; M^+ = 364.13, ^{1}H (DMSO-d6): 8.98 (2H, d, 9.3), 8.73 (2H, d, 8.2), 8.59 (2H, t, 7.9), 8.35 (1H, d, 2.3), 8.23 (3H, t, 7.4), 8.10 (2H, t, 7.5), 7.94 (1H, dd, 4.4), 7.67 (2H, dt, 7.5), 4.99 (3H, s). For **5**: k = 1.00; m.p. = 457.4 K; M^+ = 491.16; ^{1}H (CD_3CN): 1.71 and 2.42 (2H, m), 1.94 and 2.68 (2H, m), 2.26 and 2.56 (3H, s), 3.25 and 3.78 (3H, s), 3.52 and 4.31 (2H, m), 4.23 (3H, s), 6.83 (2H, d, 7.7), 7.25 (2H, d, 7.7), 7.46 (2H, d, 11.8), 7.62 (2H, m), 7.84 (2H, m), 8.26 (2H, d, 11.8). For **6**: k = 2.03; m.p. = 523.4 K; M^+ = 482.06; ^{1}H (DMSO-d6): 8.91 (2H, t, 9.4), 8.56 (1H, d, 8.6), 8.47 (1H, t, 8.6), 8.23–8.28 (2H, m), 7.67 (1H, d, 2.8), 7.25 (2H, s), 4.95 (3H, s), 4.13 (3H, s), 4.03 (6H, s). For **7**: k = 1.40; m.p. = 497.6 K; M^+ = 486.07; ^{1}H (DMSO-d6): 8.81 (2H, t, 9.0), 8.34–8.40 (2H, m), 8.17 (2H, dd, 2.8), 8.05

(1H, t, 8.5), 7.46 (1H, d,2.8), 4.86 (3H, s), 4.05 (3H, s). For **8**: k = 0.58; m.p. = 525.2 K; M^+ = 368.09; ^{1}H (DMSO-d6): 9.14 (1H, dd, 4.4), 9.01 (1H, d, 9.3), 8.60 (2H, d, 7.6), 8.42 (1H, d, 8.1), 8.29 (1H, t, 9.1), 8.15 (1H, d, 6.9), 7.37–7.42 (2H, m), 7.06 (1H, t, 6.9), 5.03 (3H, s). For **9**: k = 0.67; m.p. = 513.5 K; M^+ = 386.08; ^{1}H (CD_3CN): 8.83 (1H, dd, 5.5), 8.74 (1H, d, 9.3), 8.54 (1H, t, 7.2), 8.50 (1H, d, 8.6), 8.38 (1H, t, 7.5), 8.21 (1H, t, 7.0), 8.15 (1H, dd, 2.6), 7.28 (2H, t, 8.5), 4.94 (3H, s).

Measurements of chemiluminescence

The measurements of CL were conducted using Fluoroskan Ascent FL plate fluoroluminometer (Labsystems, Finland) set at the highest sensitivity of the detector (PMT voltage = 1000 mV) and a resolution of 20 ms per point. The samples of each CMAD (1–3 mg, Table 1) were dissolved in anhydrous *N*,*N*-dimethylformamide to assess final concentration of the acridinium salt = 5.0 mM (the stock solutions). Before the measurements, the solutions of CMADs were diluted in 1 mM HCl to obtain a concentration of 4×10^{-5} M. Next, serial dilution on a 96-well white polystyrene plate (Cliniplate) was performed (100 µl per well) to obtain a range of concentrations (10^{-5}–10^{-10} M). Next, 50 µl of 0.06% solution of H_2O_2 in 0.01 M HNO_3 were added to each well and the plate was shaken for 30 seconds. CL was triggered by adding 0.2 M aqueous solutions of base (sodium hydroxide (NaOH) or tetra-n-butylammonium hydroxide (TBAOH)). The light output was collected until the completion of light emission (up to 3-minutes). Each sample at given concentration was read 5 times; two independent samples were taken to obtain the average values.

The CL measurements of CMADs in the presence of various surfactants (cetyltrimethylammonium chloride (CTAC), *N*-dodecyl-*N*,*N*-dimethyl-3-ammonio-1-propanesulfonate (DDAPS), **4-(1,1,3,3-tetramethylbutyl)phenyl-polyethylene glycol** (Triton X-100), α-[(1,1,3,3-tetramethylbutyl)phenyl]-ω-hydroxy-poly(oxy-1,2-ethanediyl) (**Triton X-705)**) were performed essentially in the manner described above. The surfactants were added to the oxidizing solution (0.06 % H_2O_2 in 0.01 M HNO_3) in the amount to assess the optimized concentrations of 24 mM for CTAC or DDAPS and 60 mM for Triton X-100 or Triton X-705.

Values of CL decay constants (k_{CL}) were calculated as negative values of the slopes of the interdependences between natural logarithm of the value of temporary CL intensity *vs.* time. Calibration graphs were obtained by the linearization of the CL profile integrals *vs.* CMAD concentrations. The relative CL efficiencies (RCLE) for each system were obtained as the slopes of the calibration graphs. The limits of detections (LOD) and limits of

quantification (LOQ) were calculated based on the calibration graphs and known procedures, assuming a t-Student parameter set at 95% [27].

The stability of **1**–**9** in aqueous environments was assessed in the following manner: 5 mM stock solutions in DMF (see above) were diluted with Britton-Robinson buffer (pH = 8.0) or with 1 mM HCl (pH = 3.0) to reach a final concentration of each CMAD = 2.5×10^{-9} M. Aliquots (100 µl) of the above solutions were then added to 6 wells on 96-well white polystyrene plate and incubated for 30 minutes at 298 K. Next, 50 µl and 75 µl portions of 0.06 % H_2O_2 in 0.1 M HNO_3 were added to the wells containing the above acidic or alkaline solutions of CMADs (final pH was in the range of 3.0–3.5). After a 30-second shaking of the mixtures, the emission was initiated by addition 50 µl of 0.2 M NaOH (final pH = 12.5) and the total light outputs were collected by calculating the area under each kinetic profile, applying the implemented Ascent FL software.

MS and MS/MS analyses

Mass spectra of CMADs (Table 1) were recorded employing QTRAP quadrupole time-of-flight (QTOF) mass spectrometer (AB SCIEX, Canada) equipped with a duo-electrospray interface operated in positive ionization mode. MS and MS/MS operation parameters were identical for both types of scans and were as follows: the spray voltage (ISVF) was 5.5 kV, the pressure of nebulizer gas (GS1) and the heating gas (GS2) (N_2) was set at 30 psi, the curtain gas pressure (CUR) was equal to 25 psi, the sample flow rate was 20 µl min^{-1} and the source temperature was 573 K. The declustering potential (DP) was set at 100 V and the collision energy parameter (CE) was set at the value of 10. Each spectrum was obtained by averaging 3 scans; the time of each scan was 0.2 s.

For assaying the parent cations involved in **1**–**9** (Table 1), diluted solutions of CMADs in MS-grade acetonitrile (ca. 10^{-6} M) were introduced directly to the apparatus, using a 10 µl syringe (Hamilton, USA). For assaying the intermediate products of reactions of selected CMADs (**3**, **5**, **9**) with nucleophiles ($^{-}$OH and $^{-}$OOH), the solutions of the latter compounds (ca. 10^{-5} M) in 1 mM HCl were introduced as described above, followed by the addition of 10% aqueous solution of ammonia ($NH_3\times H_2O$) or the latter solution, additionally containing 1% of H_2O_2. The masses of the cationic entities (m/z), appearing in the apparatus, were recorded simultaneously with their generation, applying a flow-injection type of analysis.

Computations

All calculations were performed applying the Density Functional Theory (DFT), using the B3LYP [28] functional and the 6-31G(d,p) basis sets [29]. The unconstrained geometry optimizations for stationary points (*minima*) on the potential energy surface of investigated compounds were carried out in an aqueous solution, employing the polarizable continuum model (PCM) [30] of water in order to account for the effect of a polar environment. The validity of the geometry optimizations was confirmed in the subsequent Hessian calculations (second derivatives of the energy *vs.* atomic coordinates) followed by normal mode analyses [31]. The enthalpies and Gibbs free energies of formation of gaseous entities were obtained by applying the basic rules of thermodynamics [32]. Gaussian 09 [33] code was used for all computations, while the molecule structures were visualized with the Chemcraft package [34].

Results and Discussion

Synthesis and identity of acridinium salts (CMADs)

General methods for the preparation of derivatives of 10-methyl acridinium-9-carboxylic acid have been described in the literature [7,25,26,35]. In this work we applied an optimized routes of synthesis to obtain a series of original acridinium aryl esters (**1**–**3**, **6**, **8**, **9**, Table 1) [8] and other chemiluminogenic acridinium salts (**5**, **7**, Table 1) [10,36] (see text and Fig. S1 in SI). All the CMADs were obtained in relatively high yields and the final products were of high final purity (92.4–99.9%, Fig. S2 in SI). The introduction of substituent (F or OCH_3) in the position 2 of the acridine ring was performed by applying an optimized Ullmann-type of condensation of respective anilines and halogenobenzenes, yielding respective 4-substituted diphenylamines, further cyclized to the respective 2-substituted acridine-9-carboxylic acids [36]. The yields of last transformation were at the level of 55–80% and generally gave better results if the OCH_3 group was present in the substrate. The esterification of the acridine-9-carboxylic acids proceeded smoothly at room temperature; highly fluorinated compounds (**7**–**9**) needed 20–30% shorter times to complete the transformation as compared to the non-halogenated salts, such as **3** or **4**. On the other hand, up to 50% longer reaction times were necessary in a situation where sterically hindered phenols were involved (compounds **1**, **2**, **6**). Quaternization of the acridine-9-carboxylic acid derivatives require the use of a freshly distilled, reactive methylation reagent (methyl trifluoromethanesulfonate) and strictly dehydrated and deoxygenated conditions to obtain

high yields of products of sufficient purity (yields 75–95%). Fluorinated substrates require the use acetonitrile instead of dichloromethane or chloroform for N-methylation.

The synthesis route for obtaining activated sulfonamide salt (**5**) differs than the one applied for the acridinium esters and, generally, requires harsher conditions. The solvents have to be carefully dried to obtain an anhydrous environment, as the reagents used are highly reactive towards traces of water and the temperature of the reactions must be strictly controlled. The non-charged precursor of the sulfonamide **5** was obtained as a mixture of isomeric products that were not separated chromatographically (LC). Nevertheless, methylation of acridine N atom in the latter substrates proceeded easily with a high yield (ca. 90%) and selectively enough under optimized conditions; the final product (**5**) was isolated in a chemically pure state (ca. 95%, Fig. S2 in SI) by a through washing of the precipitate with an anhydrous diethyl ether.

The calculated masses of the parent cations of CMADs (M^+, in m/z) were verified, employing ESI-QTOF MS technique (Fig. S3 in SI). The ^{1}H NMR spectra support the assumed proton composition and structure of CMADs (Table 1), as indicated by the analysis of signals' order, integration and multiplicity. The interpretation of spectra was facilitated by our former research on that field [37]. The ^{1}H NMR spectra recorded for CMADs in DMSO-d6 or acetonitrile-d6 are presented in SI (Fig. S4). They share similarities in terms of presence of two separated regions – the aromatic region (7–9 ppm, the signals originated from the acridine and benzene rings in most compounds) and the aliphatic one, where fall the signals of aliphatic substituents, with the distinctive and characteristic singlet around 5 ppm, coming from the methyl group, attached to the endocyclic acridine nitrogen atom (N–CH_3). The spectra of the non-symmetrical fluorinated compounds (**8**, **9**) are more complicated, as ^{19}F nuclei is NMR-active due to its half spin number.

Chemiluminescence of acridinium salts in various environments

The compounds under study (CMADs) substantially differ in terms of their structure and the environment, at which the emission was triggered. As a result, the CL features of the investigated systems reflect their individual characteristics. Nevertheless, some trends and regularities can be identified and they are discussed below.

The impact of environment (the type of base, presence of surfactants) on the kinetics and CL efficiency of the acridinium salts described phenomenologically [5,7,38], but, to our knowledge, an understanding of its genesis at the molecular level is not fully recognized up to date. However, based on the former research, it can be concluded that the surfactants affect

the mechanism of light generation (especially, the "bottleneck" of CL transformations) and the observed changes do not result simply from an alteration of environmental conditions – as the surfactants have little or no effect on the fluorescence parameters of appropriate 10-methyl-9-acridinones, the target emitters during the CL of acridinium salts [39,40].

The dynamics of the CMADs' emission is reflected by the pseudo-first order kinetic constants of CL decay (k_{CL}) which are collected in Table 2 (an examples of time-dependent CL profiles are given in Fig. S5 in SI). The values of k_{CL}, obtained for all CMADs in the reference environment (plate: 0.015% H_2O_2, pH = 12.5; Table 2, row 2 from left) are characterized by large diversity and fall in the range of 10.5 s^{-1} – 0.8 s^{-1}, assuming the maximum value for the perfluorinated *tert*-butyl ester **7** and the minimum – for a sterically hindered 2,6-dimethoxy compound **6**. The other sterically hindered compound in this group, **2**, containing NO_2 group at the *para* position of the benzene ring, is surprisingly characterized by a high k_{CL} value (ca. 6.7 s^{-1} and thus – flash type of emission). The latter indicates that the influence of the strong inductive effect of the nitro group highly predominates over steric effects in this case. The change of base type – from inorganic (NaOH, typically used for CL triggering [7]) to organic tetra-n-butylammonium hydroxide (TBAOH) – is generally manifested by the increase in the dynamics of the CMADs' emission – on average by 60%. However, the typical aryl acridinium esters (with no substituent(s) in the acridinium ring, F atoms or NO_2 groups) manifest a substantial increase in k_{CL}, resultant form NaOH/TBAOH exchange – 2–3 times in the case of **1** and **4**; however, the compounds representing other types of derivatives (e.g sulfonamide **5** and perfluorinated alkyl ester **7**) behave differently in that context – as no substantial change or even a small decrease in k_{CL} were observed.

As has also been stated formerly, an ionic surfactants added to an aqueous acridinium CL systems in general positively affect the kinetics of emission [5,8,38]; in this study we observed an increase in the k_{CL} values by on average ca. 20% (DDAPS) – 50% (CTAC) (Table 2). The latter phenomenon is substantial among typical acridinium aryl esters (eg. **1**, **4**, **6**) where actual k_{CL} values are higher even by 3.0–5.5 times as compared to the reference CL system (H_2O_2/NaOH, column 2 form left, Table 2). As regards nonionic surfactants, their influence on CL dynamics is less pronounced and is negative in all cases and is most distinct in the case of sulfonamide **5**.

Summarizing the influence of environment on CL kinetics, the most sensitive CMADs for the presence of additives seem to be typical aromatic esters such as **1** or **6**, while the least sensitive in that context are the acridinium derivatives representing other types of acridinium

derivatives, such as **5** or **7**. In most cases, **7** exhibits maximum dynamics of CL decay, characterized by relatively high values of k_{CL} falling in the range of 10.5 s^{-1} (NaOH) – 4.2 s^{-1} (NaOH/CTAC), and the only acridinium sulfonamide among studied compounds (**5**) – the lowest dynamics of emission, with k_{CL} values comprised in the range of 0.5 – 0.9 s^{-1}. More significant changes in CL kinetics in the group of acridinium sulfonamides result from structural modifications of chemiluminophores themselves, as was clearly demonstrated by Adamczyk et. al [41].

The influence of environment on CMADs' relative CL efficiency (RCLE) is presented by the data summarized in Table 2; normalized RCLE values are illustrated in Figs S6 and S7 in SI. Generally, among most of the acridinium esters (**1**, **3**, **4**, **8**, **9**), a slight increase in RCLE is observed (20–30% in comparison with the reference system – column 3, Table 2), resulting from replacing the base from NaOH to TBAOH.

As regards the effect of surfactants on CMADs' RCLE, a general increase in emission efficiency (approximately 2-fold) is observed in most cases; similar statements were assumed formerly for relative systems [5,8,38]. The magnitude of this increase is generally higher in the presence of such surfactants as zwitterionic DDAPS or non-ionic Triton X-705, as compared to typical ones (cationic CTAC or non-ionic Triton X-100, respectively). Interestingly, in all cases the highest increase in RCLE was observed in the case of the compound bearing methoxy group (**6**) and the lowest (negative) change – in the case of the nitro compound **2**. The latter observation suggests a specific influence of the above-mentioned micelle-forming additives on the transformation step concerning the cleavage of the leaving group from the acridinium moiety, leading to the formation of high-energetic individuals, the immediate precursors of light emitters [7].

The changes in RCLE resulting from the presence of surfactants in CMAD-based CL systems, as referred to the reference environment are 1.0–4.8-fold for CTAC, 0.7–5.5-fold for DDAPS, 0.5–4.4-fold for Triton X-100 and 1.0–4.7-fold in the case of Triton X-705 (Table 2, column 3 from left). Generally, among studied systems, the most effective ones seem to be those based on the acridinium aromatic haloesters (especially those containing F), e.g. **1**/Triton X-705, **8**/DDAPS, while the least efficient are those based on the nitro-ester **2** and per-fluorinated aliphatic ester **7**. When comparing the sensitivity of CMADs for the introduction of surfactants into the CL system, the 2,6-dimethoxy-4-bromo compound **6**, characterized by an average 4.8-fold increase in RCLE, seems to be the most sensitive, while the least sensitive – 2,6-dimethyl-4-nitroester **2** (characterized by an average 20% decrease of

RCLE). The graph, presenting normalized values of RCLE for CMADs in various environments, is presented in SI (Fig. S7).

Unusual chemiluminogenic features of highly fluorinated derivatives presented in this work might be associated with specific features of the fluorine atom, acting as a substituent. According to this, the F atom is characterized by the highest inductive effect among all of the elements and influences the parent molecules mainly by a strong electron-withdrawing effect (–I), expressed by a high value of the inductive sigma constant (σ_I) [7,42]. On the other hand, the F atom is characterized by a positive mesomeric effect (+M), quantified by the value of resonance sigma constant, σ_R (e.g. the influence of lone pairs of electrons of F). The relative importance of the above two effects depend on the position, to which the F atom is attached. As the overall substituent effects (σ), influencing the reacting molecule can be separated into inductive and resonance contributions ($\sigma = \sigma_I + \sigma_R$), in the case of F atom, the σ overall parameter equals to 0.52 – 0.34 = 0.18 [42,43]. On the other hand, F atom expresses negligible steric effect, resulting in the fact that replacing H by F atom in an organic molecule does not significantly alter the geometry of most molecular systems. Substituent steric effects might be expressed in terms of Taft E_s parameters, assuming the values of +0.78 and +1.24, and respectively for F and H atoms. The above mentioned features of the F atom as substituent make the fluorinated compounds especially susceptible towards aromatic nucleophilic substitutions, in which the kinetics is controlled primarily by the rate of nucleophile addition. The latter is often observed in the cases of oxygen-containing nucleophiles, operating at protic, oxygen-containing solvents [43].

With regard to the limits of detection/quantification of CMADs in various environments, there is no clear interdependence observed between RCLE and LOD/LOQ values (Table 2). As the latter depend on the sort of statistical parameters – among which is the goodness of the data fit in the calibration graphs [43] and their linearity remain generally higher in the flash type systems – those based on aryl fluorinated esters in the presence of selected surfactants, such as **9**/DDAPS or **8**/Triton X-705, are characterized by the lowest LOD/LOQ values (below $2–3\times10^{-11}$ M, respectively). Generally that the LOD/LOQ assume an even order of magnitude lower values in the systems containing surfactants than in the ones with no such enhancers – in particular if the emitters are characterized by low efficiency (eg. **7**) or glow type of emission (eg. **5**).

The hydrolytic stability of CMADs, assumed as retained ability to emission of light after incubation at aqueous environments for a specified time (30 min, 298 K), were

investigated in an alkaline vs. acidic conditions (pH = 8.0 and 3.0, respectively) – where CMADs are relatively stable (Fig. S8). The results, normalized to the highest value within the data set, are presented in Fig. 1. According to that, the relative stabilities of CMADs fall in the range of 0.11–1.0, assuming the highest value for the perfluorinated alipahatic ester **7**, sulfonamide **5** and sterically hindered aryl ester **6**. On this basis we derived a parameter, named utility, being the product of the relative emission efficiency (RCLE, normalized values, Fig. S6 in SI) and the above characterized stability of compounds (Fig. 1). According to this, the CL systems of the highest utility among those investigated seem to be **1**/Triton X-705 (utility 0.74), **6**/DDAPS (utility 0.64) and **1**/CTAC ≈ **6**/CTAC (utility 0.58), while the least – those based on the nitro derivative **2** or fluorinated aryl esters **8**, **9** in all investigated environments, whose utilities fall in the range of 0.04–0.12.

As was previously shown, the target emitters upon CL of acridinium salts are respective acridan-9-ones in electronic excited states [7]. The CL spectra and the stationary fluorescence emission spectra of the respective post-reaction mixtures are essentially identical, indicating lack of subsequent processes involving the excited states. The CL spectra of acridinium salts, where the emitters are a 10-methylacridan-9-one (compounds **1**–**5**, Table 1) or 2-methoxy-10-metylacridan-9-one (**6**,**7**) were given in our former papers [7,25]. An exemplary CL emission spectrum, where the target emitter is 2-fluoro-10-methylacridan-9-one (**8**,**9**) is presented in SI (Fig. S9).

Intermediate products occurring during chemiluminescence

Research on the intermediate products appearing upon chemiluminogenic oxidation of cations involved in investigated acridinium salts ($CMADs^+$) was performed with the aid of high-resolution ESI-QTOF mass spectrometry (positive ion mode) [44]. The compounds selected for the experiments differed by the build of leaving group during the generation of light, as the latter feature mainly controls the performance of the acridinium emitters [7,8,41]. These are compound **3** – making an example of aryl ester containing no other heteroatoms instead of N and O, compound **5** – an example of sulfonamide and compound **9** – an example of highly fluorinated AE. The experiments were conducted applying a flow-injection format, enabling real-time analysis of the CL systems undergoing transformations. In each ESI-QTOF experiment, immediately after entering the volatile reactants into the tube (10% solution of $NH_3 \times H_2O$ containing 1% H_2O_2), a complex pattern of signals was obtained, which was simultaneously subjected to MS or MS/MS analysis (real-time data acquisition). Some of the

signals can be associated with the intermediate entities that have been described in the literature and were previously proposed on the basis of quantum-chemical investigations [7,8]. These products are the adducts of nucleophiles ($^{-}$OH/$^{-}$OOH or $^{\bullet}$OH/$^{\bullet}$OOH) to the reaction center, that is acridinium C9 carbon atom, starting light or dark transformations of acridinium salts in an alkaline solution of hydrogen peroxide. In particular, upon the reaction of CMADs^{+} with $NH_3 \times H_2O/H_2O_2$ mixture, acridinium adducts were observed, presumably in the form of radical-cations type CMAD(OH)$^{\bullet+}$ and CMAD(OOH)$^{\bullet+}$ (Fig 2, Table 3 and Figs S10–S12 in SI). The first type of adduct (m/z = 402.0722, Fig. 3A) can be associated with the pseudo-base form of CMAD, initiating the main dark path of CMAD transformation [8], while the hydroperoxy adduct (m/z = 419.0987, Fig. 3A) – makes the precursor of an electronically excited product, giving rise to the emission of light.

To get an insight from the viewpoint of the thermodynamics of the possibility of appearance of the above-mentioned radical cations, quantum chemical calculations of enthalpy and Gibbs free energy for the elementary steps were performed (Fig. 2A and Table 3). The analysis of precisely determined mass of cations indicates that, under experimental conditions, radical-cationic individuals type CMAD(OH)$^{\bullet+}$ and CMAD(OOH)$^{\bullet+}$ can appear on the pathway of transformations of **9** under the conditions of ESI-QTOF experiment. For the hydroxy adduct (CMAD(OH)$^{\bullet+}$) derived from compound **9** (signal of m/z ca. 402, Table 3) we have performed its MS/MS fragmentation, which indicated the appearance of characteristic fragments of m/z ca. 385 (detachment of OH), m/z 255 (detachment of 2,4,6-triPhO moiety) and m/z ca. 227 (detachment of 2,4,6-triPhOCO moiety) (Fig. S11, SI). The above adducts may appear in the system via paths I and III or V (Table 3). As regards the reaction course involving paths I–III, the process seems to be thermodynamically improbable, as one of the elementary steps, i.e. the ionization of acridane pseudobases CMAD(OH), is characterized by very highly positive values of enthalpy and Gibbs free energy (ca. 619–659 kJ mol^{-1} and 618–654 kJ mol^{-1}, respectively, Table 3). However, it must be pointed out that free electron assumed to appear on the elementary step III can be effectively stabilized with the nucleophilic molecules present in the system (H_2O, NH_3) but the energy of solvation of the free electron (at the level of 170 kJ mol^{-1} in the case of $e(H_2O)_n$ [45]) is not sufficient to compensate high ionization energy of the closed-shell molecular system assumed in step I (CMAD(OH), Table 3). On the other hand, the formation of radical cationic adducts (CMAD(OH)$^{\bullet+}$), directly by the reaction of CMADs^{+} with hydroxyl radicals ($^{\bullet}$OH) seems to be thermodynamically probable, as it is evidenced by well

negative values of free Gibbs energy, falling in the range of 154–172 kJ mol^{-1} (step V, Table 3). The radicals type $^{\bullet}OH$ or $^{\bullet}OOH$ are well known examples of reactive oxygen species (ROS), that can be formed e.g. as a result of interaction of high-energy electromagnetic radiation with water molecules [46]. Under rather extreme conditions of ESI-type ionization utilized in the MS experiments [44,47], one can expect the appearance of the above reactive individuals in the systems.

With regard to the $CMAD(OOH)^{\bullet+}$ type of adducts (hydroperoxy radical cations), also observed in the ESI-QTOF MS spectra (Figs 2A and 3A, Table 3), the thermodynamics of the elementary processes leading to their formation is similar to that for the formation of $CMAD(OH)^{\bullet+}$ radical cations discussed above (Table 3) – except that the enthalpies and Gibbs free energies for the assumed processes leading to their formation (step VI, Table 3) are significantly lower, compared to the analogical processes involving $^{\bullet}OH$ radicals (step V, Table 3). They assume values in the range of ca. –98 to –113 kJ mol^{-1} for enthalpy and –29 to –54 kJ mol^{-1} for the Gibbs free energy in gaseous phase. The results of quantum-chemical calculations remain in accordance with MS experiments, as the signals derived from $CMAD(OOH)^{\bullet+}$ are generally weaker than the ones attributed to $CMAD(OH)^{\bullet+}$. The latter indicates a lower population of the hydroperoxy adducts than the hydroxyl ones in experiment conditions (Figs S10 and S11).

What appears to be particularly interesting in the context of the mechanism of CL of $CMADs^{+}$ in aqueous alkaline media is that we were able (for exemplary compound **9**) to register a high energetic intermediate, which can be associated with a spirodioxetanone-type molecular system (in the form of $(M+1)^{+}$ pseudo-cation of m/z = 272.0731; Fig. 3B), which was suggested in former studies [4,7,8,11]. The acridane spirodioxetanones (Fig. 2B) seems to be the precursors of electronically excited 10-methyl-9-acridinones, being the final emitters in the CL process of 10-substituted acridinium salts [4,7]. The latter premise seems to be of high cognitive significance as, according to our knowledge, the existence of the above intermediate has not been demonstrated experimentally hitherto. To gain deeper insight into this problem, we performed further MS/MS fragmentation of the ion of m/z ca. 272 and observed the signals, suggesting a detachment of the moieties of H_2O (m/z 254), CO (m/z 244) and CO_2 (m/z 228) from the latter individual (Fig. 3B). These findings underline the above statements, concerning the origin of the m/z 272 signal in **9**/H_2O_2/$NH_3 \times H_2O$ system.

The ESI-QTOF MS spectrum of **9** in $NH_3 \times H_2O/H_2O_2$ mixture after reaction completion (ca. 30 seconds) simplifies significantly (Fig. S12) – it no longer contains the above-discussed

signals arisen from reaction intermediates, indicating the appearance of chemically stable [7,25] of chemiluminogenic oxidation of the AE under study; in studied case they are 2-fluoro-10-methyl-9-acridinone and 2-fluoro-10-methylacridinium-9-carboxylic acid. Their presence in the system was indicated by the occurrence of characteristic signals of m/z 228 ($(M+1)^+$) and 256, respectively. The post-CL mixture, examined after 12 hours storage in dark, presents no major differences relative to the spectrum depicted in Fig. S13 in SI.

Theoretical considerations

To better understand the processes leading to CL and to competitive dark processes (e.g. transformation of the acridinium salt to non-excited molecules of 10-methyl-9-acridinone or 9-carboxy-10-methylacridinium acid), the theoretical calculations were carried out. In the computations, all investigated CMADs were optimized at the DFT level of theory in order to investigate the Mulliken relative partial charges and the LCAO coefficients of the p_z CMADs' LUMO. The second issue to be addressed was the trend of the energy values for nucleophilic attack of $^-$OOH or $^-$OH at the endocyclic C9 atom. The thermodynamic data of the above mentioned transformations (Fig. 4A) and physicochemical features calculated for investigated compounds (Table 1) are collected in Table 4. The structures of the calculated CMAD and their Highest Occupied (HOMO) and Lowest Unoccupied (LUMO) Molecular Orbitals are presented in SI (Fig. S14).

The main molecular parameters as well as the possible pathways of the reaction of the oxidation of AEs by H_2O_2 in alkaline media leading to CL and competitive dark processes have been previously reported [4,7,8,37]. Our previous computational [7,8] as well as experimental [25] and current spectrometric investigations (see the above paragraph) on the mechanism of the oxidation of CMAD by H_2O_2 in alkaline media indicated that 10-methyl-9-acridinione, 9-carboxy-10-methylacridinium acid and phenol derivatives make the products of the reactions, mentioned above. Therefore, in this work we have focused only on the first competitive steps – nucleophilic attack of $^-$OOH (leading to the emission of radiation) or $^-$OH (creating of the 'pseudobase', leading to the dark processes) at the endocyclic C9 atom. Interest in nucleophilic attack at position 9 of acridine moiety results from the frontier orbital theory [48], which expressed that the Lowest Unoccupied Molecular Orbital (LUMO) distribution of an electrophilic species determines the molecular center sensitive to nucleophilic attack. The value of the LCAO coefficient of the p_z atomic orbital in the CMADs' LUMO is, on average, ca. 10 times higher at the endocyclic C(9) than at the C(15) carbonyl atom (0.30 and 0.03, respectively; average for investigated CMAD (**1**–**4** and **6**–**9**)

(Table 1). In the group of investigated acridinium esters, only **8** and **9** – highly fluorinated – assess the lower values of the LCAO coefficient of the p_z atomic orbital at the carbonyl atom (ratios of the LCAO coefficient of the p_z LUMO at the C9 and C15 are ca. 19 and 16, respectively). On the other hand, the sulfonamide derivative (**5**) is characterized by the highest ratio of the LCAO coefficient of the p_z LUMO at the C9 and C15 atoms among the investigated CMAD (LCAO coefficient is ca. 160 times higher at the C9 atom than at the C15). The above-mentioned results suggest that in the case of **5** the nucleophilic attack at the C15, leading to hydrolysis of the acridinium cation, is practically impossible, which was also reported in literature [7,8]. All calculated values of LCAO coefficient imply that C9 rather than the C15 marks the site of the primary nucleophilic attack of the above-mentioned anions, despite the fact that the Mulliken partial charge at C9 is lower than at the C15 atom of the carbonyl group (0.09 and 0.51, respectively; average for all investigated compounds).

Taking into account the competitive processes – leading to the CL (addition of the $^{-}$OOH) and the formation of the so-called 'pseudobase' (addition of the $^{-}$OH) – we obtain gained the thermodynamic data of these processes at the B3LYP/6–31G** level of theory (Fig. 4 and Table 4). The data indicate, that the above-mentioned steps are possible for all of the investigated compounds. The Gibbs' free energy in aqueous phase computed at temperature 298.15 K and standard pressure suggest that the addition of $^{-}$OH to C9 is thermodynamically preferred over the addition of $^{-}$OOH to the same carbon atom. In this case, the possible pathway of the reaction seems to be exclusively dependent on the kinetic factors. On the other hand, as we noted earlier [7,8] the activation barriers characterizing the addition of $^{-}$OOH or $^{-}$OH to C9 of the acridinium esters are negligible. The value of the Gibbs' free energy of the addition of $^{-}$OH at the endocyclic C9 is ca. 1.50 times lower than the Gibbs' free energy of the addition of $^{-}$OOH at the same carbon atom. In the group of investigated compounds, only in the case of **2**, **8** and **9** we observe the lower values of the above-mentioned ratio (1.41, 1.37 and 1.42, respectively). This implies that substitution with fluorine atoms in the benzene ring as well as in the acridine moiety or substitution with an electron-donor group in position 2 or 6 (or both) and simultaneously electron-acceptor group in position 4 in the phenoxy fragment increase the probability of the nucleophilic attack of the $^{-}$OOH at the C9 atom of the acridinium esters, leading to the CL. On the other hand, in the case of compound **6** (2,6-dimethoxy and 4-bromo-substituent in the benzene ring) we did not observe such an effect. This may be the result of substitution with an electron-donor group in the position 2 of the acridinium moiety.

Fig. 4B illustrates the probable location of the nucleophilic attack ($^{-}$OH or $^{-}$OOH) as it flows from the above analysis of p_z LUMO orbitals, of C9 and C15 acridnium atoms characterized by the deficiency of electronic charge. Interestingly, the ratio of C9 to C15 LCAO p_z LUMO coefficients (C9/C15), expressing the difference between the susceptibility of both places to the nucleophilic attack, remain in a positive linear relationship with experimentally derived values of the kinetic constants (k_{CL}) characterizing CL decay in the family of acridnium aryl esters.

Conclusions

A series of original chemiluminogenic acridinium salts (CMADs, Table 1), representing various classes of acridine-9-carboxylic acid derivatives (aromatic and aliphatic esters and representative sulfonamide) were synthesized with high yields, isolated in a pure form (>92%) and identified by means of elemental analysis, RP-HPLC as well as ^{1}H NMR and ESI-QTOF MS spectroscopy.

In general, most of CMADs investigated in aqueous environments perform advantageously in terms of their chemiluminogenic properties (kinetics and efficiency of emission, stability) if compare to unsubstituted acridinium phenyl ester, characterized before [7]. Highly fluorinated aromatic esters, the perfluorinated aliphatic ester as well as the acridinium sulfonamide behave individually in that context. Chemiluminogenic features of CMADs-based systems are altered in the presence of selected surfactants, added at the optimized amounts to the aqueous light-triggering systems (Table 2). In particular, zwitterionic surfactants such as DDAPS and non-ionic as Triton X-705, significantly enhance the light output (2–5 times), expressed by relative values of emission efficiency (RCLE). The ionic surfactants such as CTAC or DDAPS increase the time course of emission – as evidenced by 2–3 higher values of CL decay kinetic constant values (k_{CL}), while the non-ionic ones, such as Triton X-100 and Triton X-705, do not alter or even diminish emission time. No relationship was observed between the RCLE and the k_{CL} values, among studied CL systems.

In most cases, the perfluorinated *tert*-butyl ester **7** exhibits maximum dynamics of CL decay, characterized by k_{CL} values falling in the range of 10.5–4.2 s^{-1}, and the only acridinium sulfonamide in this group **5** – the lowest dynamics of emission, with k_{CL} values comprised in the range of 0.5–0.9 s^{-1}. Hence, the latter compound seems to be of the lowest sensitivity to the properties of environment. Halogenated aryl esters **1** and **8** make the most efficient emitters among studied CL systems (the most efficient are: **1**/Triton X-705,

8/DDAPS), while **2** and **7** – seem to be the least efficient. Compound **5** is characterized by moderate or low RCLE in aqueous environment if compared to other investigated CMADs.

The analysis of the stability of CMADs revealed that compounds **5** and **7** retain almost complete ability to emission after incubation in an alkaline buffer (30 min., 298 K), while the fluorinated aryl esters (**8** and **9**) show a mere 11–16% of the initial efficiency under the same conditions (Fig. 1). Sterically hindered and activated at the *para* position of the benzene ring aryl esters **1** and **6** also express high stability, at the level of 80%. The product of relative stability and CL efficiency of given CMAD, named utility, assumes the highest values in the cases of aqueous CL systems comprising compound **1** and Triton X-705 or DDAPS, **6**/DDAPS or Triton X-705 and **5**/Triton X-100 or Triton X-705. The latter parameter can be used for assessing the utility of a given acridinium-based system in analytics.

ESI-QTOF MS experiments performed with the participation of representative CMADs in the flow injection mode enabled us to observe the hydroxyl and hydroperoxy adducts in the environment of $NH_3 \cdot H_2O/H_2O_2$ mixture – presumably in the form of radical cations type $CMAD(OH)^{\bullet+}$ and $CMAD(OOH)^{\bullet+}$ (Figs 2 and 3). According to the quantum chemistry calculations (DFT level of theory), the latter individuals are formed under experimental conditions as a result of the attack of hydroxyl or hydroperoxide radicals onto the C9 atom of the acridinium cation ($CMAD^+$) (Table 3). In the case of the compound **9** we were able to detect and perform MS/MS fragmentation of the acridan spirodioxetanone – the individual, making the immediate precursor of electronically excited product giving rise to CL. To our knowledge, the latter finding makes the first experimental evidence for the existence of this high-energetic entity on the pathways of chemiluminogenic oxidation of acridinium salts.

The DFT-calculated LCAO coefficients of the p_z LUMO orbitals at the acridinium C9 and C15 atoms suggest, that in the group of investigated compounds C9 carbon makes the center of the nucleophilic attack (Table 4, Fig. 4A). The C9/C15 ratios, indicating the difference in the susceptibilities to nucleophilic attack on both atoms in the group of aryl esters, remain in positive linear relationship with the kinetics constants of CL decay (Fig. 4B).

Acknowledgements

This work was financed by the National Scientific Center (NCN) through grants No. 2011/03/D/ST4/02419 (contract No. UMO-2011/03/D/ST4/02419) and 2012/05/B/ST5/01680 (contract No. UMO-2012/05/B/ST5/01680). Calculations were carried out on the computers of the Wroclaw Centre for Networking and Supercomputing (WCSS) (grant No. 215).

References

[1] A. Wróblewska, O.M. Huta, S.V. Midyanyj, I.O. Patsay, J. Rak, J. Błażejowski, Origin of chemiluminescence accompanying the reaction of the 9-cyano-10-methylacridinium cation with hydrogen peroxide, J. Org. Chem. 69 (2004) 1607–1614.

[2] A. Wróblewska, O.M. Huta, I.O. Patsay, R.S. Petryshyn, J. Błażejowski, Addition of nucleophiles to the 9-cyano-10-methylacridinium cation: utilization in their chemiluminescent assay, Anal. Chim. Acta 507 (2004) 229–236.

[3] F. McCapra, Chemical mechanisms in bioluminescence, Acc. Chem. Res. 9 (1976) 201–208.

[4] J. Rak, P. Skurski, J. Blazejowski, Toward an understanding of the chemiluminescence accompanying the reaction of 9-carboxy-10-methylacridinium phenyl ester with hydrogen peroxide, J. Org. Chem. 64 (1999) 3002–3008.

[5] A. Natrajan, D. Sharpe, D. Wen, Effect of surfactants on the chemiluminescence of acridinium dimethylphenyl ester labels and their conjugates, Org. Biomol. Chem. 9 (2011) 5092–5103.

[6] A. Natrajan, D. Sharpe, D. Wen, Chemiluminescence from alkoxy-substituted acridinium dimethylphenyl ester labels, Org. Biomol. Chem. 10 (2012) 3432–3447.

[7] K. Krzymiński, A. Ożóg, P. Malecha, A.D. Roshal, A. Wróblewska, B. Zadykowicz, J. Błażejowski, Chemiluminogenic features of 10-methyl-9-(phenoxycarbonyl)acridinium trifluoromethanesulfonates alkyl substituted at the benzene ring in aqueous media, J. Org. Chem. 76 (2011) 1072–1085.

[8] B. Zadykowicz, J. Czechowska, A. Ożóg, A. Renkevich, K. Krzymiński, Effective chemiluminogenic systems based on acridinium esters bearing substituents of various electronic and steric properties, Org. Biomol. Chem. 14 (2016) 652–668.

[9] M. Adamczyk, Y.-Y. Chen, P.G. Mattingly, Y. Pan, S. Rege, Neopentyl 3-triflyloxypropanesulfonate. A reactive sulfopropylation reagent for the preparation of chemiluminescent labels, J. Org. Chem. 63 (1998) 5636–5639.

[10] M. Adamczyk, Y.-Y. Chen, P.G. Mattingly, J.A. Moore, K. Shreder, Modulation of the chemiluminescent signal from N10-(3-sulfopropyl)-N-sulfonylacridinium-9-carboxamides, Tetrahedron 55 (1999) 10899–10914.

[11] F. McCapra, Chemiluminescence of organic compounds, Pure Appl. Chem. 24 (1970) 611–629.

[12] C. Dodeigne, L. Thunus, R. Lejeune, Chemiluminescence as diagnostic tool. A review, Talanta 51 (2000) 415–439.

[13] L.J. Kricka, Clinical applications of chemiluminescence, Anal. Chim. Acta. 500 (2003) 279–286.

[14] A. Roda, M. Guardigli, E. Michelini, M. Mirasoli, P. Pasini, Analytical bioluminescence and chemiluminescence, Anal. Chem. 1 (2003) 462A–470A.

[15] S. Baj, T. Krawczyk, Chemiluminescence detection of organic peroxides in a two-phase system, Anal. Chim. Acta 585 (2007) 147–153.

[16] A.M. García–Campaña, F.J. Lara, Trends in the analytical applications of chemiluminescence in the liquid phase, Anal. Bioanal. Chem. 387 (2007) 165–169.

[17] L. Gámiz–Gracia, A.M. García–Campaña, J.F. Huertas–Pérez, F.J. Lara, Chemiluminescence detection in liquid chromatography: Applications to clinical, pharmaceutical, environmental and food analysis. A review, Anal. Chim. Acta 640 (2009) 7–28.

[18] L. Zhao, L. Sun, X. Chu X, Chemiluminescence immunoassay, Trends Anal. Chem. 28 (2009) 404–415.

[19] F. Watanabe, S. Takenaka, K. Abe, Y. Tamura, Y. Nakano, Comparison of a microbiological assay and a fully automated chemiluminescent system for the determination of vitamin B_{12} in food, J. Agric. Food Chem. 46 (1998) 1433–1436.

[20] L. Gámiz–Gracia, A.M. García–Campaña, J.J. Soto–Chinchilla, J.F. Huertas Pérez, A. González Casado, Analysis of pesticides by chemiluminescence detection in the liquid phase, Trends Anal. Chem. 24 (2005) 927–942.

[21] J.S.A. Simpson, A.K. Campbell, M.E.T. Ryall, J.S. Woodhead, A stable chemiluminescent-labelled antibody for immunological assays, Nature 279 (1979) 646–647.

[22] R.C. Brown, Z. Li, A.J. Rutter, X. Mu, O.H. Weeks, K. Smith, I. Weeks, Development and application of a novel acridinium ester for use as a chemiluminescent emitter in nucleic acid hybridisation assays using chemiluminescence quenching, Org. Biomol. Chem. 7 (2009) 386–394.

[23] A. Natrajan, D. Sharpe, J. Costello, Q. Jiang, Enhanced immunoassay sensitivity using chemiluminescent acridinium esters with increased light output, Anal. Biochem. 406 (2010) 204–213.

[24] I. Weeks, I. Beheshti, F. McCapra, A.K. Campbell, J.S. Woodhead, Acridinium esters as high-specific-activity labels in immunoassay, Clin. Chem. 29 (1983) 1474–1479.

[25] K. Krzymiński, A.D. Roshal, B. Zadykowicz, A. Białk-Bielińska, A. Sieradzan, Chemiluminogenic properties of 10-methyl-9-(phenoxycarbonyl)acridinium cations in organic environments, J. Phys. Chem. 114 (2010) 10550–10562.

[26] N. Sato, Synthesis and properties of new luminescent 10-carboxymethylacridinium derivatives, Tetrahedron Lett. 37 (1996) 8519–8522.

[27] P.C. Meier, R.E. Zünd, Statistical methods in analytical chemistry, Wiley, New York, 2000.

[28] (a) A.D. Becke, A new mixing of Hartree-Fock and local-density functional theories, J. Chem. Phys. 98 (1993) 1372–1377; (b) A.D. Becke, Density-functional thermochemistry. III. The role of exact exchange, J. Chem. Phys. 98 (1993) 5648–5652.

[29] (a) R. Ditchfield, W.J. Hehre, J.A. Pople, Self-consistent molecular-orbital methods. IX. An extended Gaussian-type basis for molecular-orbital studies of organic molecules, J. Chem. Phys. 54 (1971) 724–728; (b) W.J. Hehre, R. Ditchfield, J.A. Pople, Self-consistent molecular orbital methods. II. Further extensions of Gaussian-type basis sets for use in molecular orbital studies of organic molecules, J. Chem. Phys. 56 (1972) 2257–2261.

[30] (a) S. Miertuš, E. Scrocco, J. Tomasi, Electrostatic interaction of a solute with a continuum. A direct utilizaion of Ab initio molecular potentials for the prevision of solvent effects, Chem. Phys. 55 (1981) 117–129; (b) S. Miertuš, J. Tomasi, Approximate evaluations of the electrostatic free energy and internal energy changes in solution processes, Chem. Phys. 65 (1982) 239–245; (c) M. Cossi, V. Barone, R. Cammi, J. Tomasi, Ab initio study of solvated molecules: a new implementation of the polarizable continuum model, Chem. Phys. Lett. 255 (1996) 327–335.

[31] W.J. Hehre, L. Radom, P.R. von Schleyer, A. Pople, Ab initio molecular orbital theory, Wiley, N.Y., 1986.

[32] P. Atkins, J. de Paula, Physical Chemistry, 9th ed., Freeman WH, Oxford, 2009.

[33] M.J. Frisch, G.W. Trucks, H.B. Schlegel, G.E. Scuseria, M.A. Robb, J.R. Cheeseman, G. Scalmani, V. Barone, B. Mennucci, G.A. Petersson, H. Nakatsuji, M. Caricato, X. Li, H.P. Hratchian, A.F. Izmaylov, J. Bloino, G. Zheng, J.L. Sonnenberg, M. Hada, M. Ehara, K. Toyota, R. Fukuda, J. Hasegawa, M. Ishida, T.

Nakajima, Y. Honda, O. Kitao, H. Nakai, T. Vreven, J.A. Montgomery Jr, J.E. Peralta, F. Ogliaro, M. Bearpark , J.J. Heyd, E. Brothers, K.N. Kudin, V.N. Staroverov, T. Keith, R. Kobayashi, J. Normand, K. Raghavachari, A. Rendell, J.C. Burant, S.S. Iyengar, J. Tomasi, M. Cossi, N. Rega, J.M. Millam, M. Klene, J.E. Knox, J.B. Cross, V. Bakken, C. Adamo, J. Jaramillo, R. Gomperts, R.E. Stratmann, O. Yazyev, A.J. Austin, R. Cammi, C. Pomelli, J.W. Ochterski, R.L. Martin, K. Morokuma, V.G. Zakrzewski, G.A. Voth, P. Salvador, J.J. Dannenberg, S. Dapprich, A.D. Daniels, O. Farkas, J.B. Foresman, J.V. Ortiz, J. Cioslowski, D.J. Fox, Gaussian 09, Revision D.01. Gaussian, Inc., Wallingford CT, 2013.

[34] G.A. Zhurko, D.A. Zhurko, Chemcraft Version 1.8 (built 426), http://www.chemcraftprog.com, 2014.

[35] A. Sikorski, K. Krzymiński, A. Niziołek, J. Błażejowski, 9-(2,6-Difluorophenoxycarbonyl)-10-methylacridinium trifluoromethanesulfonate and its precursor 2,6-difluorophenyl acridine-9-carboxylate: C–H···O, C–F···π, S–O···π and π–π stacking interactions, Acta Crystallogr. C61 (2005) o690–o694.

[36] G. Zomer, J.F.C. Stavenuiter, Chemiluminogenic labels, old and new, Anal. Chim. Acta 227 (1989) 11–19.

[37] K. Krzymiński, P. Malecha, B. Zadykowicz, A. Wróblewska, J. Błażejowski, ^{1}H and ^{13}C NMR spectra, structure and physicochemical features of phenyl acridine-9-carboxylates and 10-methyl-9-(phenoxycarbonyl)acridinium trifluoromethanesulphonates – alkyl substituted in the phenyl fragment, Spectrochim. Acta A. 78 (2011) 401–409.

[38] A. Natrajan, D. Wen, Use of degradable cationic surfactants with cleavable linkages for enhancing the chemiluminescence of acridinium ester labels, RSC Adv. 3 (2013) 21398–21404.

[39] W.L. Hinze, T.E. Riehl, H.N. Singh, Y. Baba, Micelle-enhanced chemiluminescence and application to the determination of biological reductants using lucigenin, Anal. Chem. 56 (1984) 2180–2191.

[40] B.K. De, E. Jimenez, S. De, J.C. Sawyer, G.A. McMillin, Analytical performance characteristics of the Abbott Architect i2000 Tacrolimus assay; comparisons with liquid chromatography-tandem mass spectrometry (LC-MS/MS) and Abbott IMx methods, Clin. Chim. Acta 410 (2009) 25–30.

[41] M. Adamczyk, P.G. Mattingly, Chemiluminescent N-sulfonylacridinium-9-carboxamides and their application in clinical assays, in: K. Van Dyke, C. Van Dyke, K. Woodfork (Eds.), Luminescence Biotechnology: Instruments and Applications, CRC Press, Boca Raton, 2001, pp. 77–105.

[42] T. Siodła, W.P. Ozimiński, M. Hoffmann, H. Koroniak, T.M. Krygowski, Toward a physical interpretation of substituent effects: the case of fluorine and trifluoromethyl groups, J. Org. Chem. 79 (2014) 7321−7331.

[43] R.D. Chambers, The Influence of Fluorine or Fluorocarbon Groups on Some Reaction Centres, in Fluorine in Organic Chemistry, Blackwell Publishing Ltd., Oxford, 2004, UK. 91−121.

[44] User Guide: DuoSpray Ion Source for TripleTOF Systems Operator Guide, https://sciex.com/x34163, 2014, (accessed: 27.09.16).

[45] B. Abel, U. Buck, A.L. Sobolewski, W. Domcke, On the nature and signatures of the solvated electron in water, Phys. Chem. Chem. Phys. **14** (2012) 22–34.

[46] J.H. Baxendale, J. A. Wilson, The photolysis of hydrogen peroxide at high light intensities, **Trans. Faraday Soc. 53** (1957) 344–356.

[47] M. Adamczyk, J.R. Fishpaugh, J.C. Gebler, P.G. Mattingly, K. Shreder, Letter: Detection of reaction intermediates by flow injection electrospray ionization mass spectrometry: reaction of chemiluminescent *N*-sulfonylacridinium-9-carboxamides with hydrogen peroxide, Eur. J. Mass Spectrom. 4 (1998) 121−125.

[48] I. Fleming, Frontier Orbitals and Organic Chemical Reactions, Wiley, London, New York, 1976.

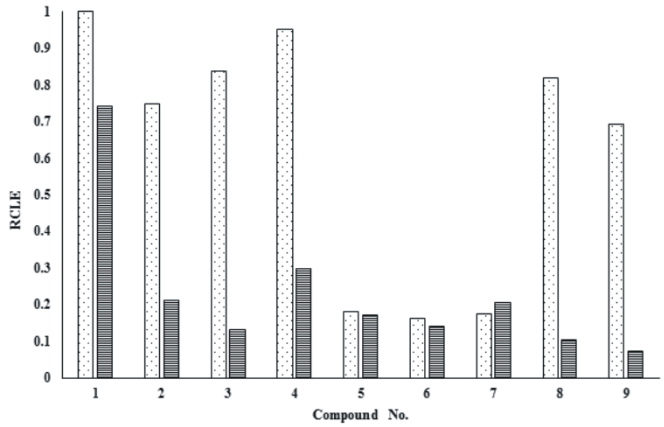

Fig. 1. Relative chemiluminescence efficiency (RCLE, normalized integral data) of CMADs (Table 1), recorded after incubation (30 min., 298 K) of acridinium salt in acidic (pH = 3.0, light bars) or alkaline (pH = 8.0, dark bars) environments. For details see the Experimental section.

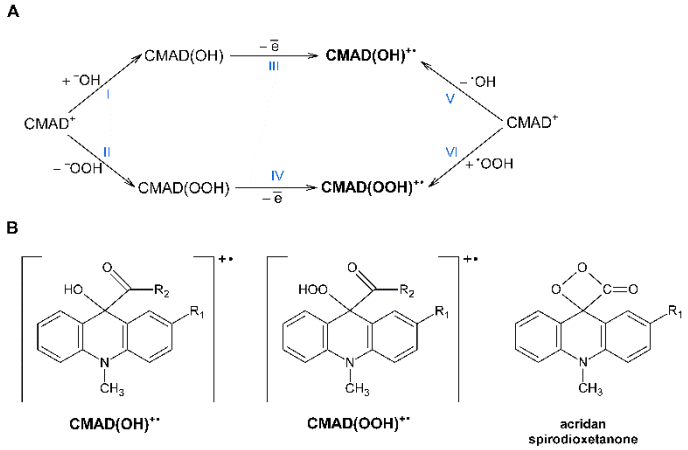

Fig. 2. A: Theoretically investigated pathways (see Table 3) leading to the formation of radical cationic adducts of CMADs (Table 1); **B**: Canonic structures of intermediates assumed to be formed with the participation of CMADs and $NH_3 \times H_2O/H_2O_2$ mixture, observed in flow-injection ESI-QTOF MS experiments (positive-mode of acquisition).

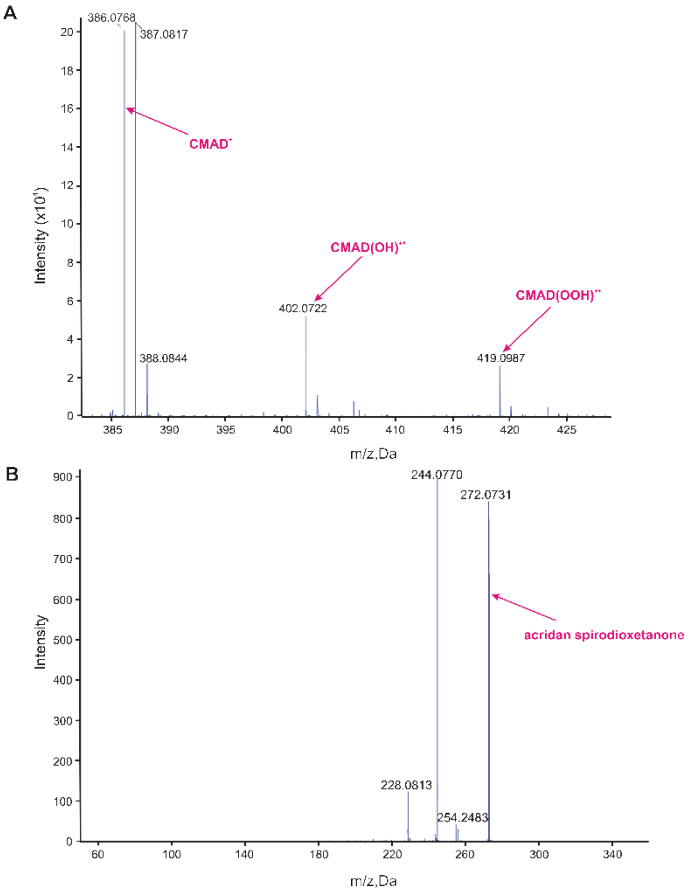

Fig. 3. A: The signals of hydroxy- and hydroperoxy- radical cationic adducts (CMAD(OH)$^{\bullet+}$ and CMAD(OOH)$^{\bullet+}$, respectively) formed with the participation of **9** (Table 1) in $NH_3 \times H_2O/H_2O_2$ environment under flow-injection ESI-QTOF MS experiment (see also Table 3 and Fig. 2); **B**: The positive mode MS signals of acridan spirodioxetanone intermediate (as $[M+1]^+$ pseudocation, see Fig. 2B) and its fragmentation ions, observed durin transformations of **9** in $NH_3 \times H_2O/H_2O_2$ environment under flow-injection conditions of ESI-QTOF MS experiment. For details see the Experimental section.

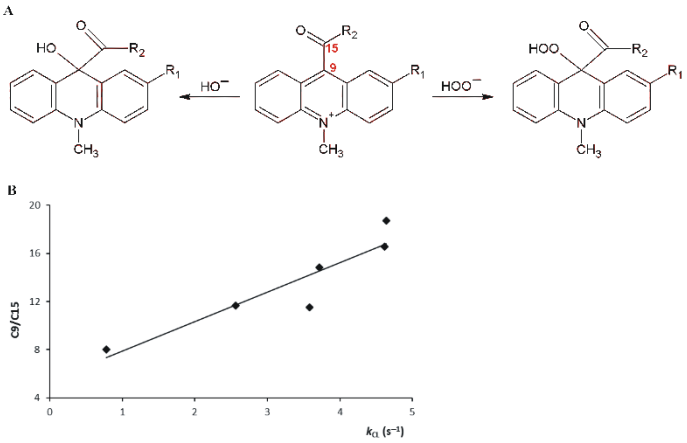

Fig. 4. A: Probable location of nucleophilic attack of OH^- or OOH^- ions onto the acridinium cations ($CMADs^+$), as flows from the analysis of pz LUMO orbitals characterizing C9 and C15 atoms (marked in red); **B**: Interdependence between the ratios of LCAO coefficients of the pz LUMO orbitals of C9 and C15 atoms (C9/C15) and the pseudo-first order kinetics constants of CL decay (k_{CL}) for CMADs representing acridnium aryl ester sub-group (**1**, **3**, **4**, **6**, **8**, **9**, Table 1). The line correspond to the following equation: $C9/C15 = 2.448 \cdot k_{CL} + 5.4274$ ($R^2 = 0.90$).

Table 1. Structural formula and systematic names of the 9-carboxy-10-methylacridinium derivatives (CMADs) investigated.

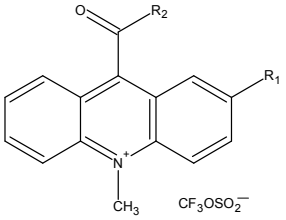

compound number	substituent R_1	substituent R_2	name of the cation involved ($CMAD^+$)
1	H	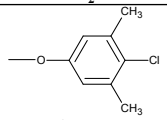	9-[(4-chloro-3,5-dimethylphenoxy)carbonyl]-10-methylacridinium
2	H	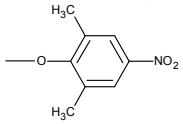	9-[(2,6-dimethyl-4-nitrophenoxy)carbonyl]-10-methylacridinium
3	H	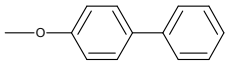	9-[(biphenyl-4-yloxy)carbonyl]-10-methylacridinium
4	H	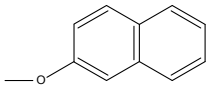	10-methyl-9-[(naphthalen-2-yloxy)carbonyl]acridinium
5	H	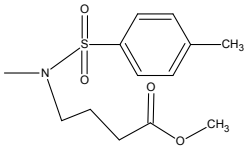	9-[[(4-methoxy-4-oxobutyl)-[(4-methylphenyl)sulfonyl]amino]carbonyl]-10-methylacridinium
6	OCH_3	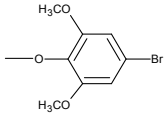	9-[(4-bromo-2,6-dimethoxyphenoxy)carbonyl]-2-methoxy-10-methylacridinium
7	OCH_3	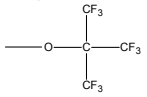	9-({[1,1,1,3,3,3-hexafluoro-2-(trifluoromethyl)propan-2-yl]oxy}carbonyl)-2-methoxy-10-methylacridinium
8	F	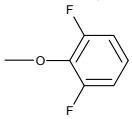	9-[(2,6-difluorophenoxy)carbonyl]-2-fluoro-10-methylacridinium
9	F	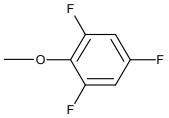	2-fluoro-10-methyl-9-[(2,4,6-trifluorophenoxy)carbonyl]acridinium

Table 2. Chemiluminescence parameters obtained for CMADs (Table 1) assessed in optimized environments (H_2O_2/surfactants/NaOH) and apparatus setup (maximal sensitivity of PMT). Lower values in columns 2–4 from left were obtained with the participation of organic base (TBAOH) instead of NaOH. Presented data are the average values (n = 3) obtained for two independent samples. The coefficients of variation (CV) for the presented data fall in the range of 1–8%. For details see the Experimental section.

cpd No.	no surfactant			CTAC			DDAPS			Triton X-100			Triton X-705		
	k_{CL}	RCLE $\times10^{11}$	LOD/LOQ $\times10^{-10}$	k_{CL}	RCLE $\times10^{11}$	LOD/LOQ $\times10^{-10}$	k_{CL}	RCLE $\times10^{11}$	LOD/LOQ $\times10^{-10}$	k_{CL}	RCLE $\times10^{11}$	LOD/LOQ $\times10^{-10}$	k_{CL}	RCLE $\times10^{11}$	LOD/LOQ $\times10^{-10}$
1	2.56 7.99	4.39 3.65	1.55/2.44 0.872/1.40	6.07	6.91	0.971/1.51	4.67	7.26	0.450/0.715	2.25	5.98	1.44/2.24	2.67	8.78	1.18/1.83
2	6.67 3.81	2.41 1.32	0.344/0.555 2.12/3.29	5.47	2.72	0.546/0.840	6.34	1.79	0.633/0.990	5.49	1.20	0.346/0.546	0.73	2.41	0.553/0.858
3	3.58 6.82	3.76 3.01	1.74/2.72 0.453/0.727	3.67	2.74	1.17/1.83	2.08	4.62	0.803/1.25	1.30	3.73	1.81/2.82	2.24	7.02	1.57/2.45
4	3.72 8.63	3.33 4.40	1.49/2.33 1.81/2.86	3.50	5.17	0.454/0.712	5.13	6.78	0.350/0.545	1.61	5.06	1.21/1.89	2.18	6.51	2.41/3.81
5	0.85 0.87	2.30 1.51	10.7/17.0 9.62/15.0	0.81	2.84	3.88/6.05	0.45	2.93	3.33/5.20	0.76	5.05	1.44/2.24	0.68	4.47	1.18/1.83
6	0.78 1.44	1.21 3.66	16.2/25.2 2.83/4.45	4.32	5.85	0.520/0.886	2.35	6.42	1.62/2.71	0.13	5.22	2.93/4.80	0.14	5.72	5.70/8.90
7	10.48 8.38	1.19 0.67	46.2/72.1 1.17/1.80	4.19	2.34	0.968/1.48	7.55	2.44	1.26/1.94	6.17	2.41	1.53/2.37	4.81	2.46	0.820/1.28
8	4.64 5.53	3.20 3.90	1.20/1.87 0.666/1.03	2.71	6.22	0.431/0.671	4.72	8.54	0.370/0.576	5.45	7.22	0.395/0.642	0.88	8.05	0.220/0.359
9	4.62 5.79	2.45 3.15	1.96/3.02 0.667/1.07	5.63	5.26	0.797/1.24	4.25	6.61	0.172/0.271	3.17	3.85	1.42/2.20	1.01	4.38	1.64/2.54

TBAOH – denotes tetra-n-butylammonium hydroxide; CTAC – cetyltrimethylammonium chloride; DDAPS – N,N-dimethyldodecylammonio-1,3-propane sulfonate; Triton X-100 – 4-(1,1,3,3-Tetramethylbutyl) phenyl-polyethylene glycol; Triton X-705 – α-[(1,1,3,3-Tetramethylbutyl)phenyl]-ω-hydroxy-poly(oxy-1,2-ethanediyl); k_{CL} – denotes the CL decay pseudo-first order kinetic constant (in s^{-1}); RCLE – denotes the relative chemiluminescence efficiency; LOD/LOQ – the limit of detection and the limit of quantification (in M), respectively.

Table 3. Thermodynamic data characterizing elementary steps leading to the formation of intermediate radical-cationic adducts (CMAD(OH) $^{\bullet+}$ and CMAD(OOH)$^{\bullet+}$, Fig. 2) upon the reaction of selected CMADs (**3**, **5**, **9**, Table 1) with $NH_3 \times H_2O/H_2O_2$ mixture. First column from right present signals observed in ESI-QTOF experiments (flow-injection mode). Values in parentheses denote the m/z values of fragmentation ions. For details see the Experimental section.

step no. (Fig. 2)	compound no.	elementary process	$\Delta_{r,298}H^o$	$\Delta_{r,298}G^o$	main cations observed (ESI-QTOF MS, m/z)
I	**3**	$CMAD^+ + {}^-OH \rightarrow CMAD(OH)$	–790.7	–748.4	
	5		–778.5	–729.2	
	9		–812.8	–769.5	
II	**3**	$CMAD^+ + {}^-OOH \rightarrow CMAD(OOH)$	–698.5	–642.8	
	5		–675.4	–616.6	
	9		–699.2	–645.9	
III	**3**	$CMAD(OH) - \bar{e} \rightarrow CMAD(OH)^{\bullet+}$	618.9	618.1	
	5		624.4	629.3	
	9		642.1	640.5	
IV	**3**	$CMAD(OOH) - \bar{e} \rightarrow CMAD(OOH)^{\bullet+}$	643.2	640.4	
	5		634.1	639.3	
	9		659.2	653.5	
V	**3**	$CMAD^+ + {}^{\bullet}OH \rightarrow CMAD(OH)^{\bullet+}$	–171.8	–130.3	406.1395, 407.1428
	5		–154.1	–99.8	507.1555, 508.1585
	9		–170.7	–129.0	402.0717 (374.0381, 385.3446, 227.0755)
VI	**3**	$CMAD^+ + {}^{\bullet}OOH \rightarrow CMAD(OOH)^{\bullet+}$	–113.2	–53.9	423.1657, 424.1696
	5		–99.1	–28.8	524.1819, 525.1825
	9		–97.8	–43.9	419.0983

$\Delta_{r,298}H^o$ and $\Delta_{r,298}G^o$ (in kJ mol^{-1}), respectively, represent the enthalpy and Gibbs' free energy in gaseous phase of the reaction corresponding to a given step number at temperature 298.15 K and standard pressure.

Table 4. Thermodynamic data and physicochemical features of investigated CMADs obtained using the B3LYP/6–31G** level of theory. See also Fig. 4.

cpd no. (Table 1)	$\Delta_{r,298}G^o$ in aqueous phase [a]		LCAO coefficient of the pz LUMO at		Mulliken partial charge at	
	OOH^-	OH^-	C9	C15	C9	C15
1	–180.6	–260.7	0.3099	0.0266	0.0938	0.5132
2	–186.2	–263.6	0.2940	0.0352	0.0916	0.5203
3	–181.8	–260.1	0.3078	0.0267	0.0937	0.5143
4	–182.9	–268.8	0.3184	0.0215	0.0948	0.5145
5	–165.5	–246.4	0.2088	0.0013	0.0496	0.5154
6	–165.0	–247.1	0.2922	0.0364	0.0782	0.5330
7	–175.0	–257.1	0.2999	0.0334	0.0873	0.5053
8	–188.4	–259.2	0.3108	0.0166	0.0937	0.5006
9	–188.4	–266.9	0.3110	0.0188	0.0930	0.4997

[a] $\Delta_{r,298}G^o$ represent the Gibbs' free energy in aqueous phase of the reaction of addition of the acridinium cation ($CMAD^+$) with ^-OOH or ^-OH at T = 298.15 K and standard pressure. All thermodynamic data are in kJ mol^{-1}.

Supplementary Information

Chemiluminogenic acridinim salts: a comparison study. Detection of intermediate entities appearing upon light generation

Justyna Czechowska, Alicja Kawecka, Anna Romanowska,
Maria Marczak, Paweł Wityk, Karol Krzymiński* and Beata Zadykowicz*

Faculty of Chemistry, University of Gdańsk, Wita Stwosza 63, 80–308 Gdansk, Poland

* Correspondence to: Faculty of Chemistry, University of Gdansk, Wita Stwosza 63, 80–308 Gdansk, Poland. E-mail: karol.krzyminski@ug.edu.pl (K. Krzymiński), beata.zadykowicz@ug.edu.pl (B. Zadykowicz).

Synthesis of chemiluminogenic acridnium salts (CMADs)

Substituted 9-[(phenoxy)carbonyl]-10-methylacridinium trifluoromethanesulfonates (aryl acridinium esters **1**–**4**, **6**, **8**, **9** (Table 1) were synthesized in four steps, accordingly to our previous works [8,25] (Fig. S1A).

General procedure for the synthesis of ring-substituted acridine-9-carboxylic acid (step I)

A solution of 1 mmol of 4-substituted-*N*-phenylaniline in dichloromethane (750 μl) was added dropwise over 15 minutes to a solution of 1 mmol of oxalyl chloride in dry dichloromethane (190 μl). The solution was refluxed for 1 h, then volatiles were evaporated, and the residue was redissolved in 500 μl of dichloromethane. The cooled solution was treated with 3.7 mmol of $AlCl_3$, added in portions. The solution was refluxed for 1.5 h. The volatiles were removed and the residue was quenched with a mixture of ice and aqueous solution of HCl (c = 1 mol dm^{-3}) (v/v = 1:1.6). Orange isatin derivative was filtered and dried. Without further purification, the isatin derivative was refluxed with 2.6 ml of 10 % aqueous solution of KOH for 24 h, cooled, evaporated, and quenched with the mixture of aqueous solution of HCl (c = 5 mol dm^{-3}) and ice (v/v = 3:1). The yellow product was filtered. 2-Fluoroacridine-9-carboxylic acid: yield 55%; 2-methoxyacridine-9-carboxylic acid: yield 83%.

Unsubstituted acridine-9-carboxylic acid was purchased from *Sigma-Aldrich*.

General procedure for the synthesis of 9-(chlorocarbonyl)acridinium chloride (step II)

The solution of dehydrated acridine-9-carboxylic acid derivative in excess of thionyl chloride was refluxed for 3 h. $SOCl_2$ was evaporated and crude product was washed with dry toluene. 9-(chlorocarbonyl)acridinium chloride derivatives (unsubstituted, 2-fluoro- and 2-methoxy-) were obtained quantitatively.

General procedure for the synthesis of esterification of 9-(chlorocarbonyl)acridinium chloride (step III)

To the solution of 1 mmol 9-(chlorocarbonyl)acridinium chloride derivative in dichloromethane were added 3-fold molar excess of *N*,*N*,*N*-triethylamine and catalytic amounts of *N*,*N*-(dimethyl)-4-aminopyridine (DMAP). After few minutes the corresponding phenol derivative (0.75 mmol) was added. The solution was stirred for 15–40 hours at room temperature, then diluted with dichloromethane (25 ml) and 3 times washed with water (12 ml). The organic layer was dried over magnesium sulphate, filtered and concentrated. Product was purified by gravitational LC chromatography (stationary phase: SiO2; mobile phase: ethyl acetate/hexane (v/v 1/2). Yields: 50–80 %.

General procedure for the synthesis of 10-methylacridinium trifluoromethanesulphonate derivatives (step IV)

To a solution of 1 mmol of an acridine derivative in 5 ml dry dichloromethane were added catalytic amount of polymer-bound 2,6-di*tert*-butylpyridine and 10 molar excess of methyl trifluoromethanesulphonate. The solution was stirred at room temperature for 4 h. The precipitate was filtered off and washed with dichloromethane. The filtrate was evaporated under vacuum at room temperature to 5 ml and diluted with diethyl ether. The precipitate was filtered and vacuum-dried.

*The synthesis of 9-[[(4-methoxy-4-oxobutyl)-[(4-metyhylphenyl)sulfonyl]amino]carbonyl-10-metyloacridinium triflоromethanesulphonate (***5***)*

Compound **5** was synthesized according to the modification of described procedure [9,10] (Fig. S1B). A portion of 4-aminobutyrate hydrochloride (1 mmol) was stirred with a stechiometric quantity of *para*-toluenesulfonylchloride in chloroform (6 ml) in the presence of *N*,*N*-dimethylamine under argon. The reaction mixture was cooled in ice bath (ice + NaCl) while *para*-toluensulfonylchloride was added. Reaction mixture was stirred for 24 h in room temperature. Product was purified by extraction with 5 % aqueous solution of sodium hydrogen carbonate. Organic extract was dried over anhydrous magnesium sulphate and purified by gravitational LC chromatography (stationary phase: SiO_2, mobile phase: methanol/chloroform (1/19 v/v). Yield: ca. 50%. Next, 1 mmol of methyl *N*-tosyl-4-aminobutyrate was stirred with sodium hydride (2 mmol) and 9-(chlorocarbonyl)acridinium chloride (1 mmol) in tetrahydrofuran and presence of *N*,*N*-dimethylamine under argon. Reaction mixture was cooled in ice bath (ice + NaCl) and new portion of sodium hydride (2 mmol) was added. Reaction mixture was stirred for 3 h in room temperature. Product was dissolved in chloroform (100 ml) and extracted with water. Organic extract was dried over anhydrous magnesium sulphate and purified by gravitational LC chromatography (stationary phase: SiO_2, mobile phase: ethyl acetate/cyclohexane (3/7 *v*/*v*). Yield: 51 %. 9-[[(4-methoxy-4-oxobutyl)-[(4-metyhylphenyl)sulfonyl]amino]carbonyl]acridine was converted to 10-methylacridinium quaternary salt according to the procedure for aryl acridnium esters described above. Yield: 78%.

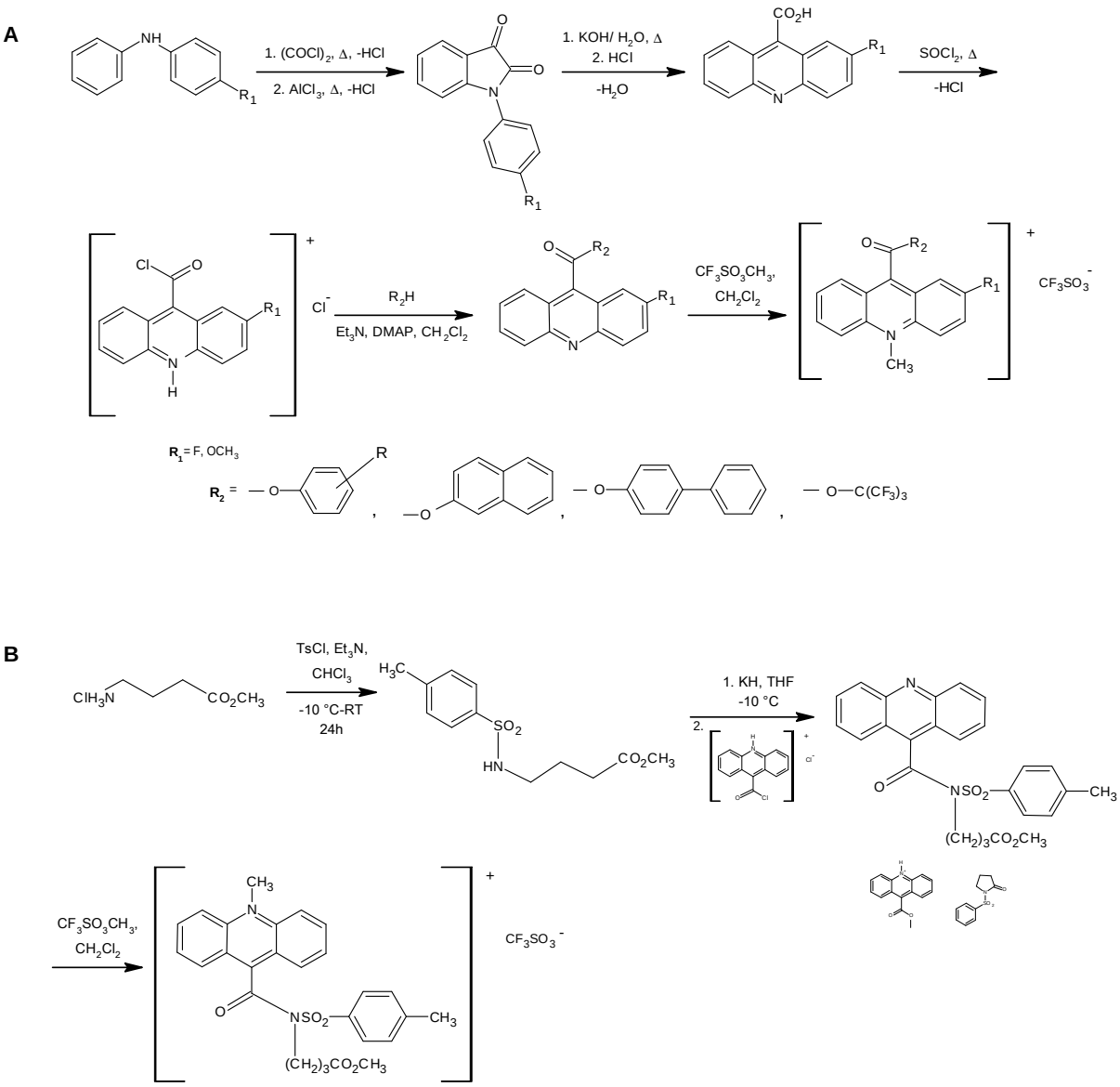

Fig. S1. A: Synthesis route for 9-[(aryloxy)carbonyl]-10-methylacridinium triflates (aromatic acridinium esters substituted in benzene and acridine rings). **B**: Synthesis route for 9-[[(4-methoxy-4-oxobutyl)-[(4-metyhylphenyl) sulfonyl]amino]carbonyl-10-metyloacridinium (acridinium sulfonamide).

Cpd No.	chromatogram at 254 nm (exemplary)	Purity (%)*
1	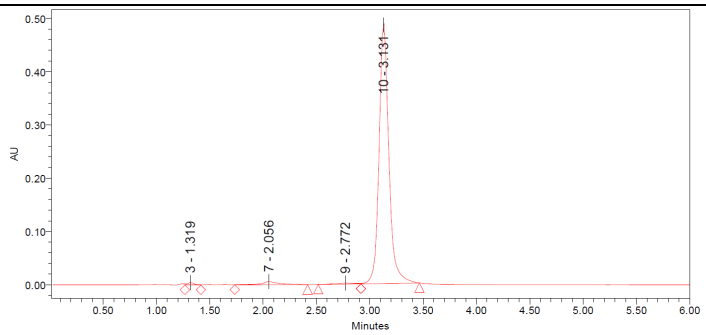	96.5
2	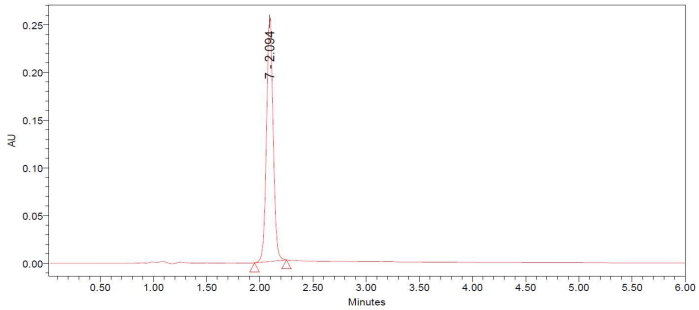	>99%
3	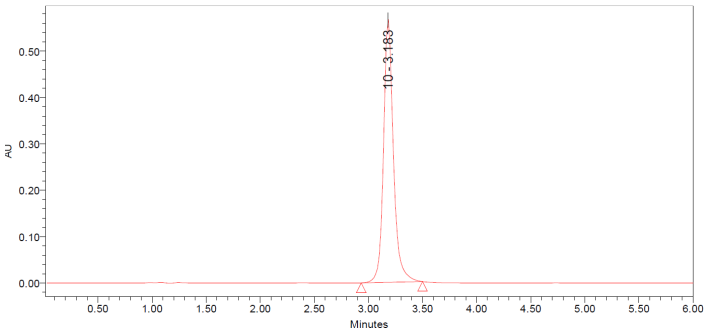	>99%
4	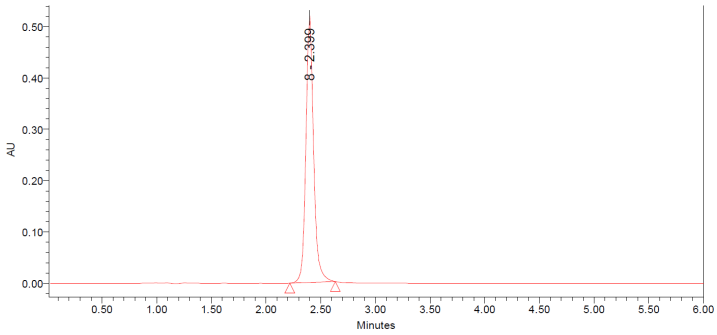	>99%
5	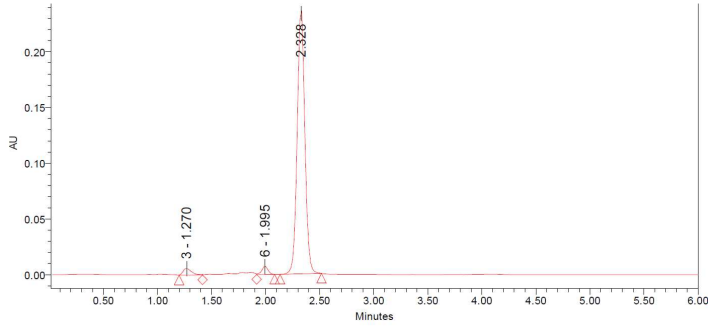	94.9%

6	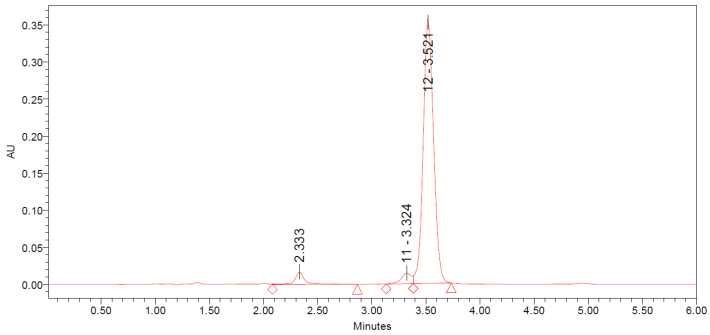	92.4
7	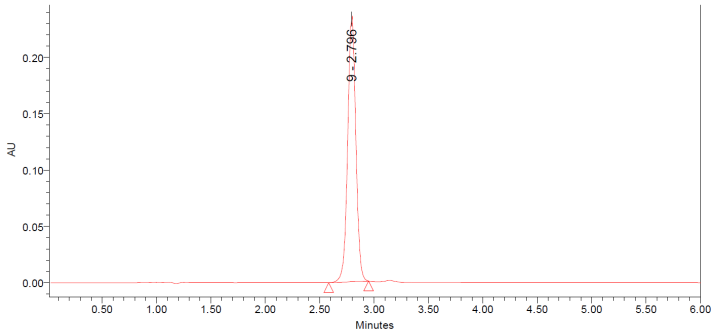	>99%
8	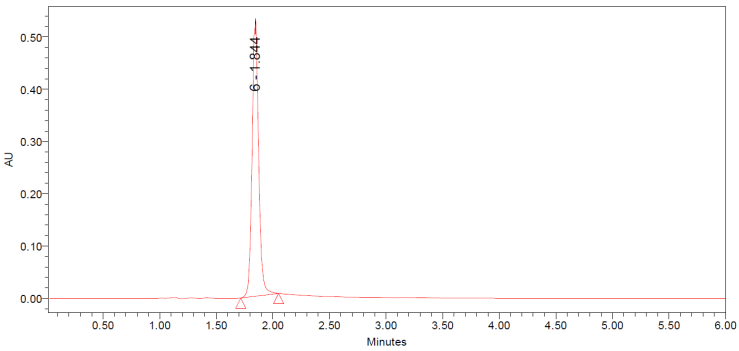	>99%
9	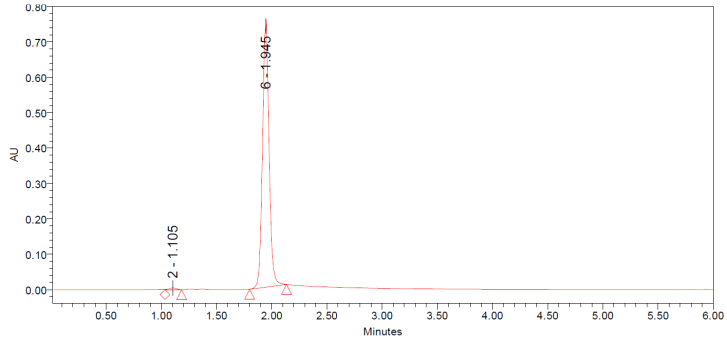	99.4

*calculated as area under the main signal, average value from 254/365 nm detectors.

Fig. S2. RP-HPLC analyses of compounds investigated (CMADs, Table 1). Experimental conditions, kept constant in all analyses, were as follows: stationary phase: Gemini 5µ C6-Phenyl 110A, 100×4.6 mm column (Phenomenex); mobile phase: isocratic, 1 ml/min, acetonitrile/0.1% TFA in water – 1/1 v/v; absorbance detection at 254 nm and 365 nm. For details see Experimental section.

cpd no.	ESI-QTOF MS spectrum (positive mode)	cations detected (found/calculated, in m/z)
1	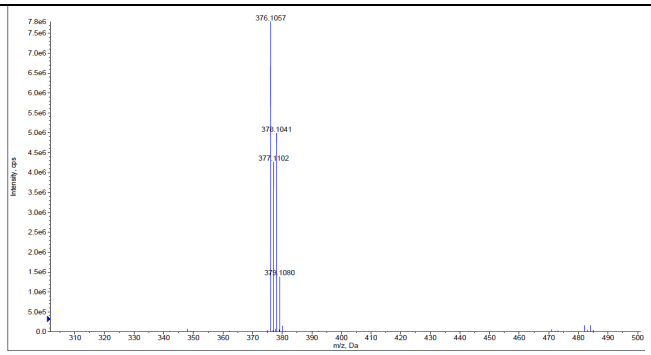	376.1057 / 376.11 ($M^+ = C_{23}H_{19}ClNO_2^+$)
1, fragmentation	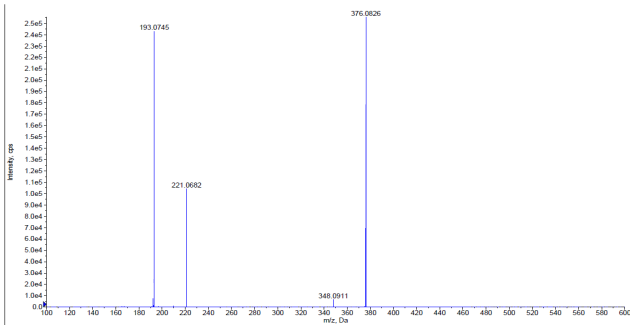	
2	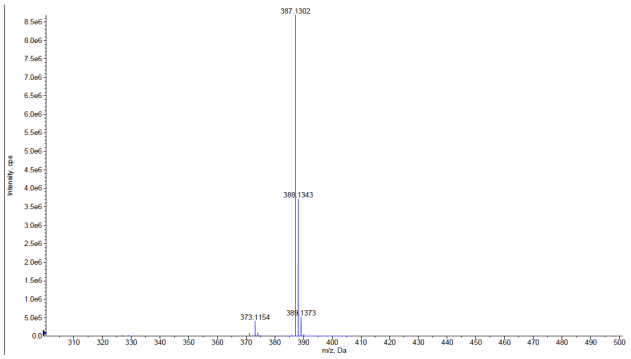	387.1302 / 387.13 ($M^+ = C_{23}H_{19}N_2O_4^+$)
2, fragmentation	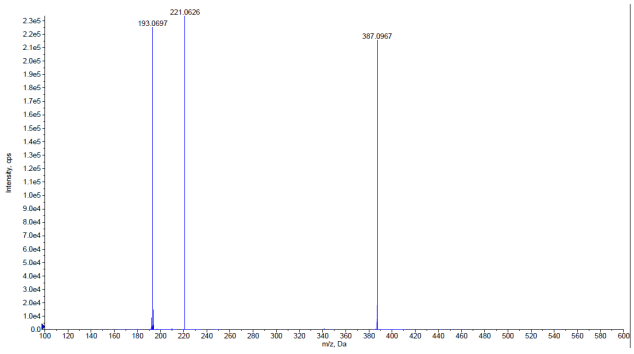	

3

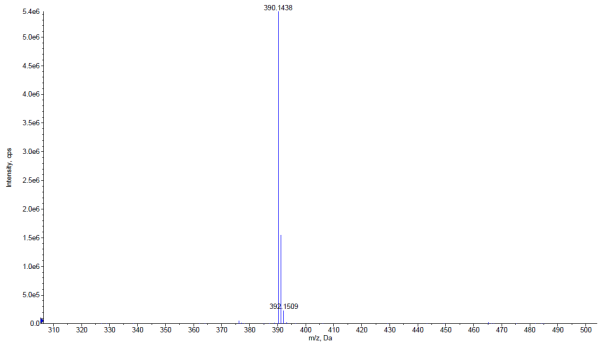

390.1438 / 390.15

($M^+ = C_{27}H_{20}NO_2^+$)

3,

fragmentation

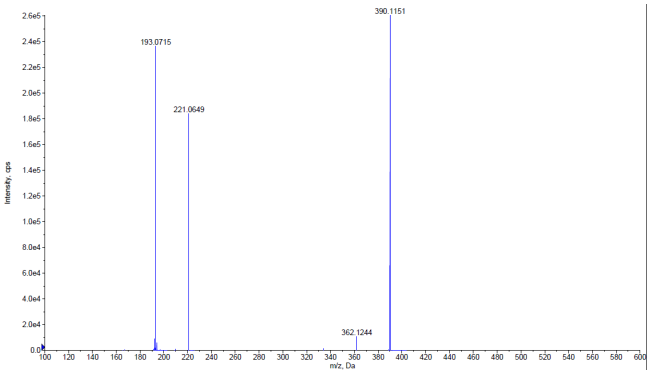

4

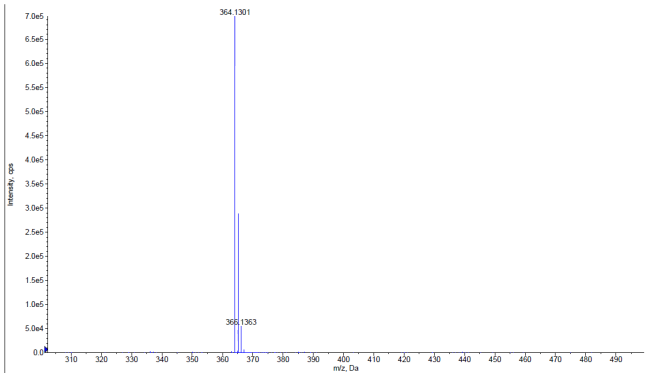

364.1301 / 364.13

($M^+ = C_{25}H_{18}NO_2^+$)

4,

fragmentation

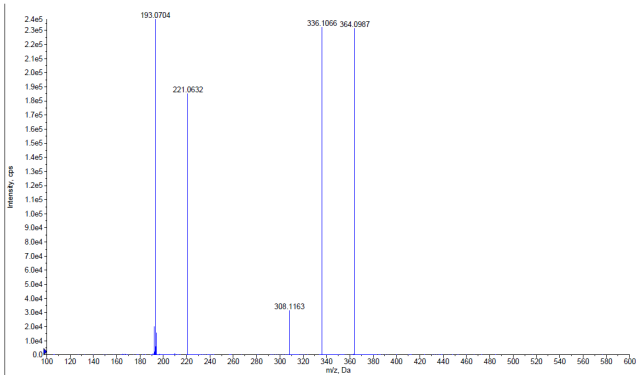

5

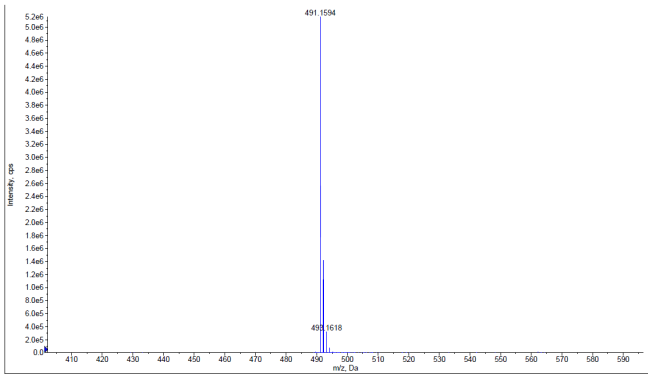

491.1594 / 491.16

($M^+ = C_{27}H_{27}N_2O_5S^+$)

5,

fragmentation

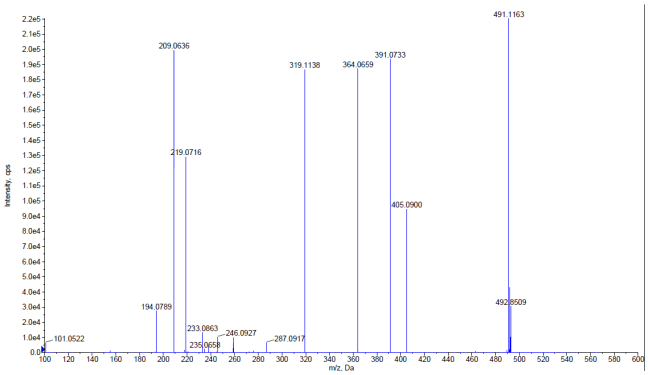

6

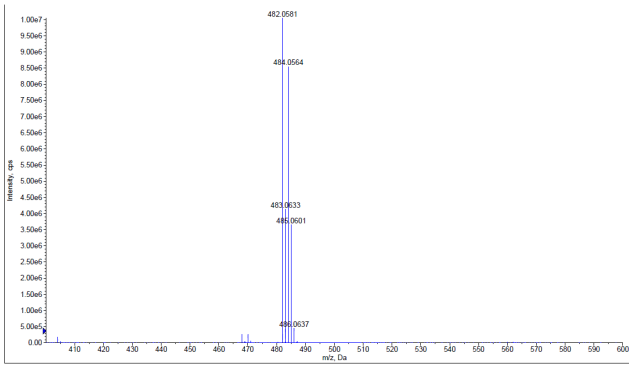

482.0581 / 482.06

($M^+ = C_{24}H_{21}BrNO_5^+$)

6,

fragmentation

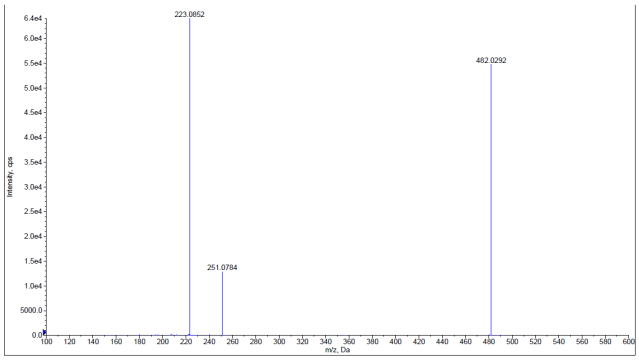

7

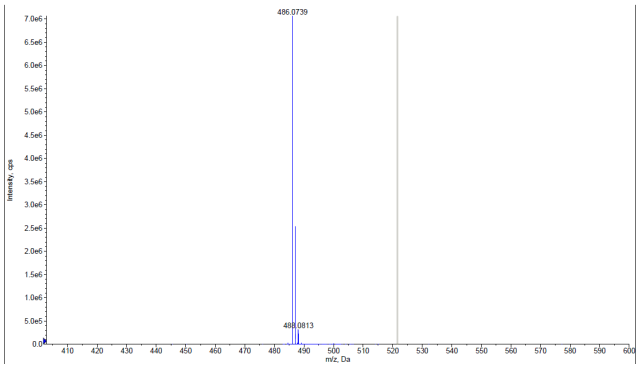

486.0739 / 486.07

($M^+ = C_{20}H_{13}F_9NO_3^+$)

7,

fragmentation

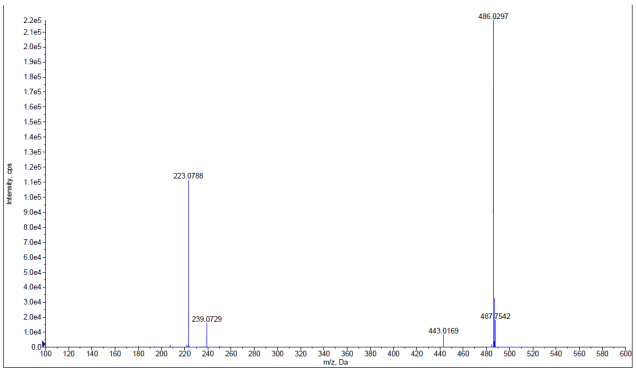

8

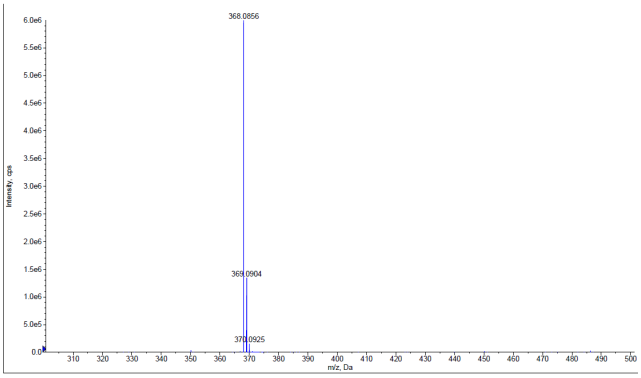

368.0856 / 368.09

($M^+ = C_{21}H_{13}F_3NO_2^+$)

8,

fragmentation

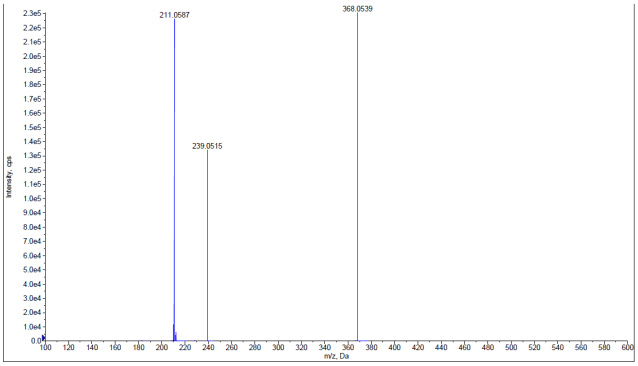

9	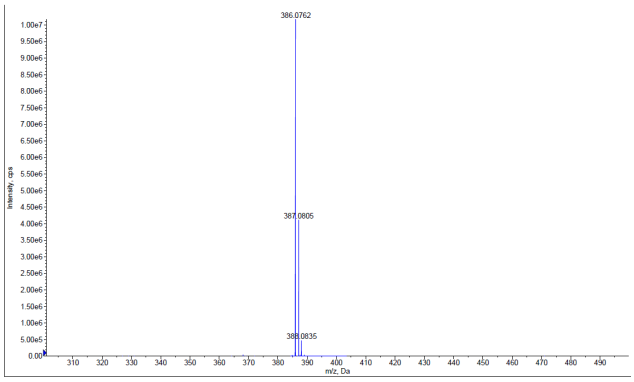	386.0762 / 386.08 ($M^+ = C_{21}H_{12}F_4NO_2^+$)
9, fragmentation	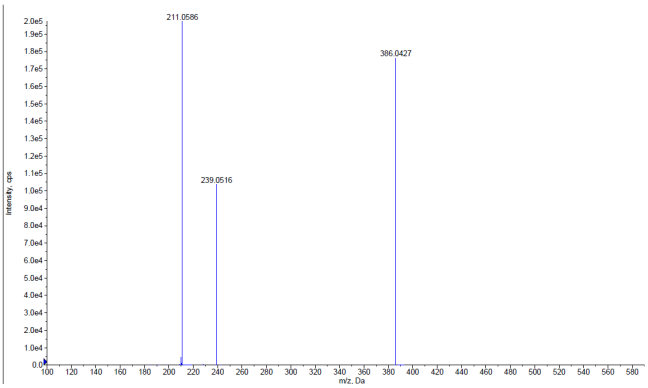	

Fig. S3. ESI-QTOF MS spectra (positive mode of acqusition) of the parent monocations, involved in acridinium salts investigated ($CMADs^+$, Table 1). Conditions: TripleTOF™ 5600^+ MS spectrometer (AB Sciex, Canada), GS1 = GS2 = 30 psi, CUR = 25 psi, TEM = 300˚C, ISVF = 5500 V, CE = 10, DP = 100, V = 20 ml min^{-1}. Samples, dissolved in acetonitrile (MS grade, 20 µl) were introduced directly, using glass syringe (Hamilton, USA). For details see the Experimental part.

cpd no.	^{1}H NMR spectrum
1 aromatic region	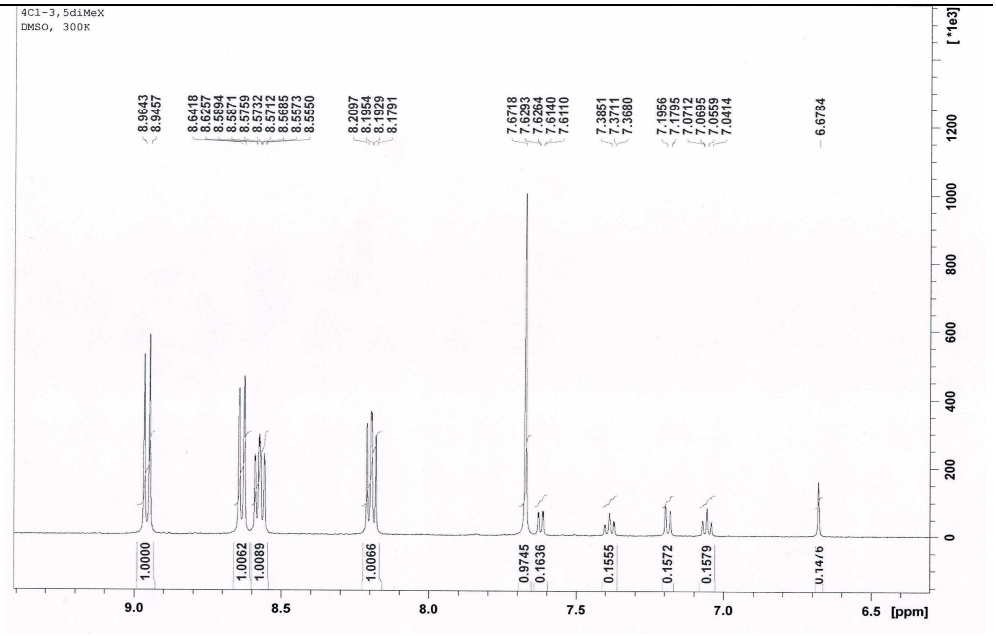
1 aliphatic region	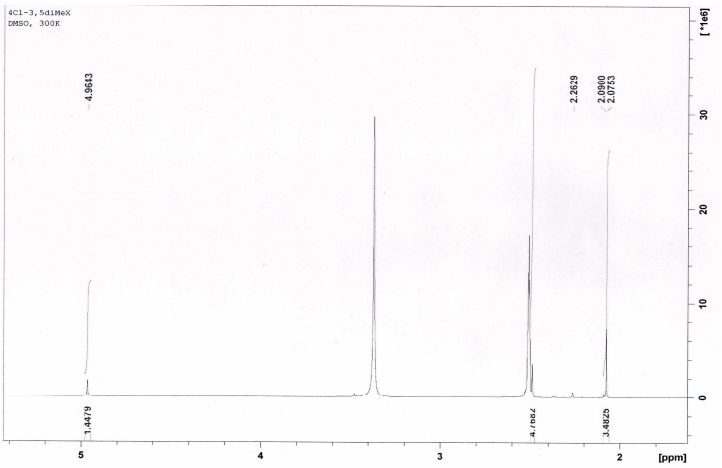

2
aromatic
region

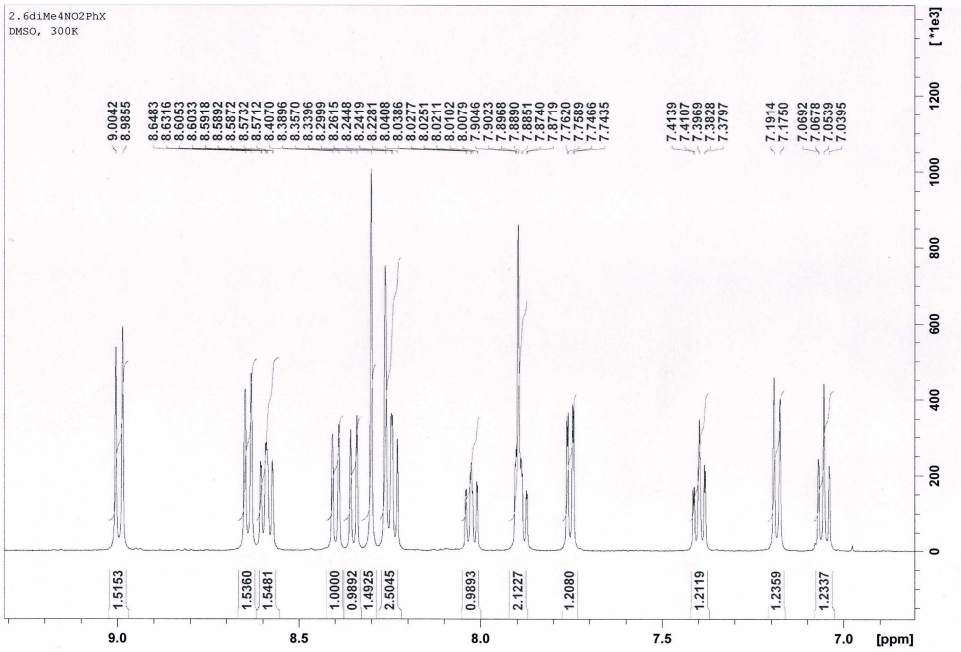

2
aliphatic
region

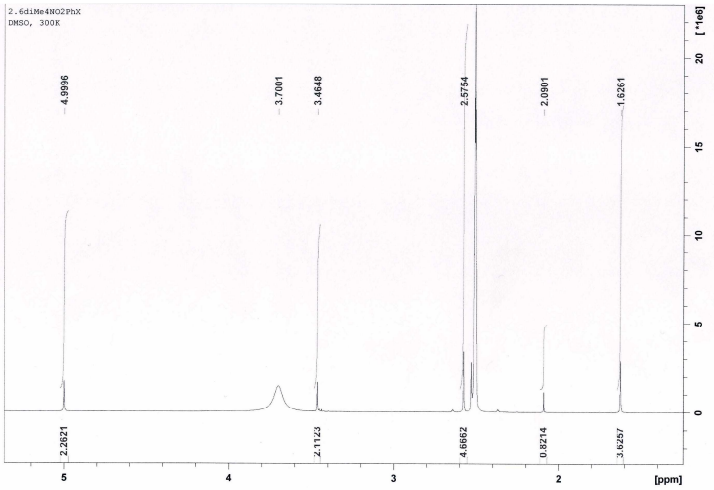

3
aromatic
region

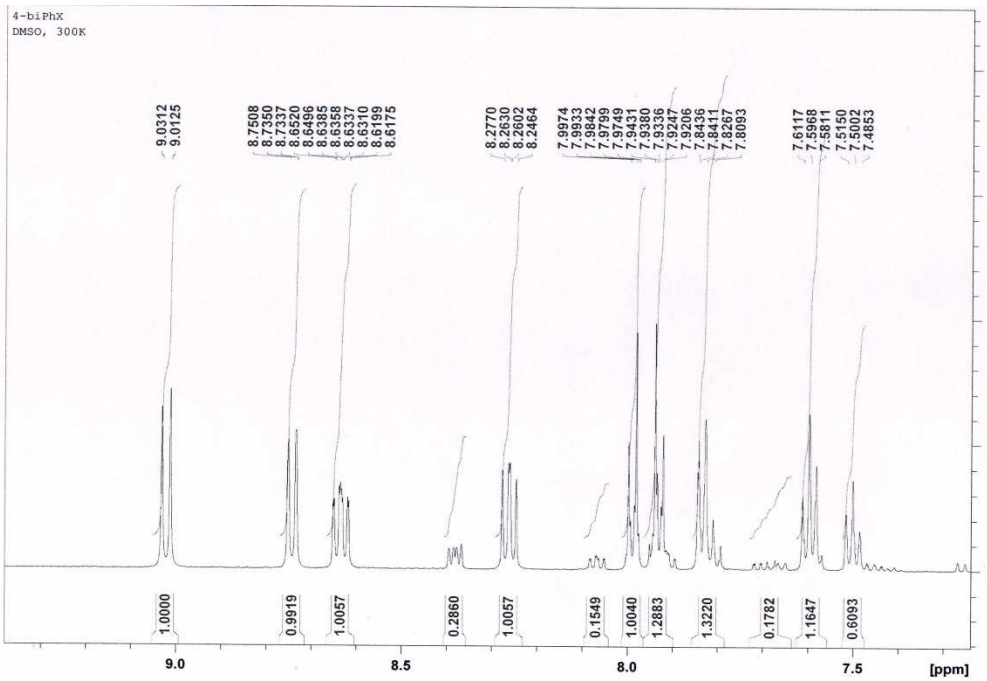

3

aliphatic

region

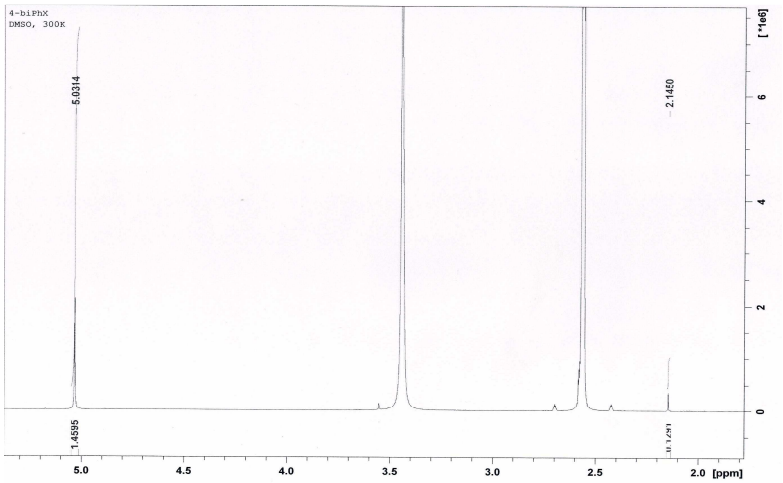

4

aromatic

region

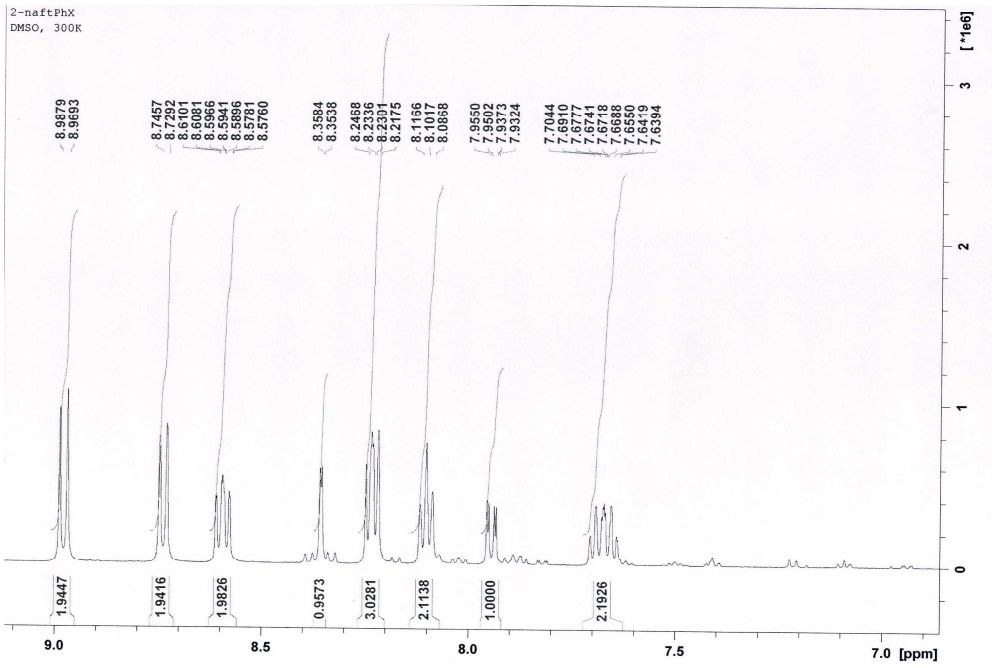

4

aliphatic

region

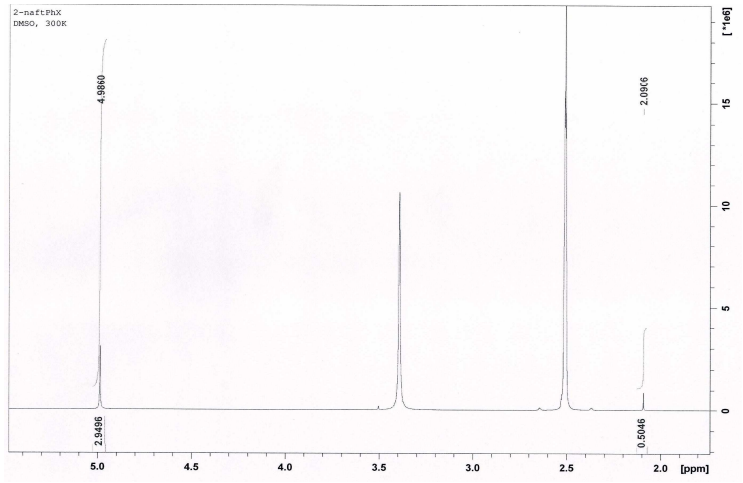

5

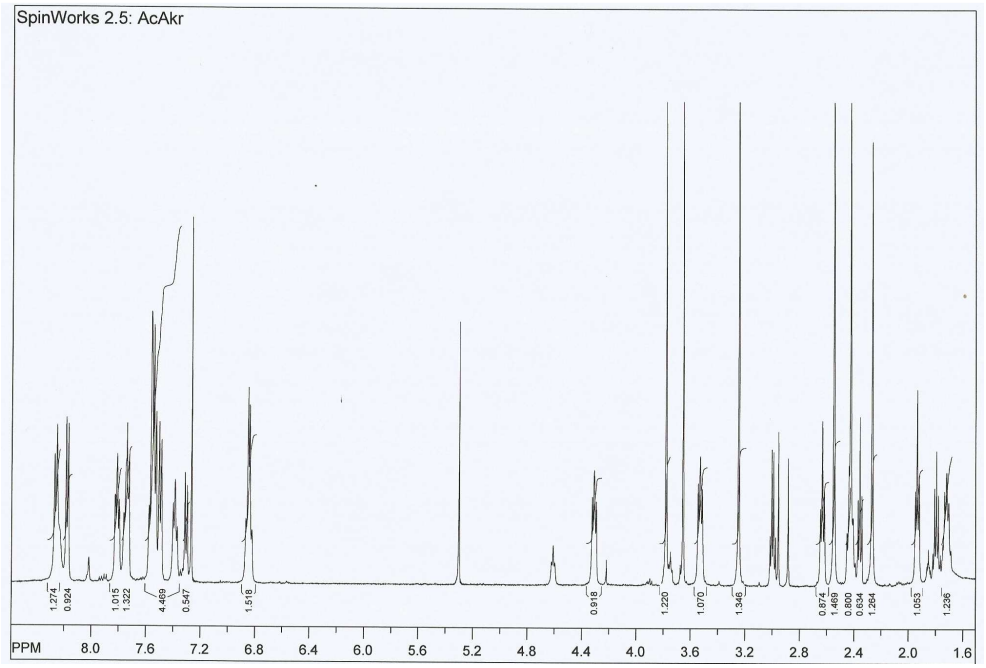

6

aromatic region

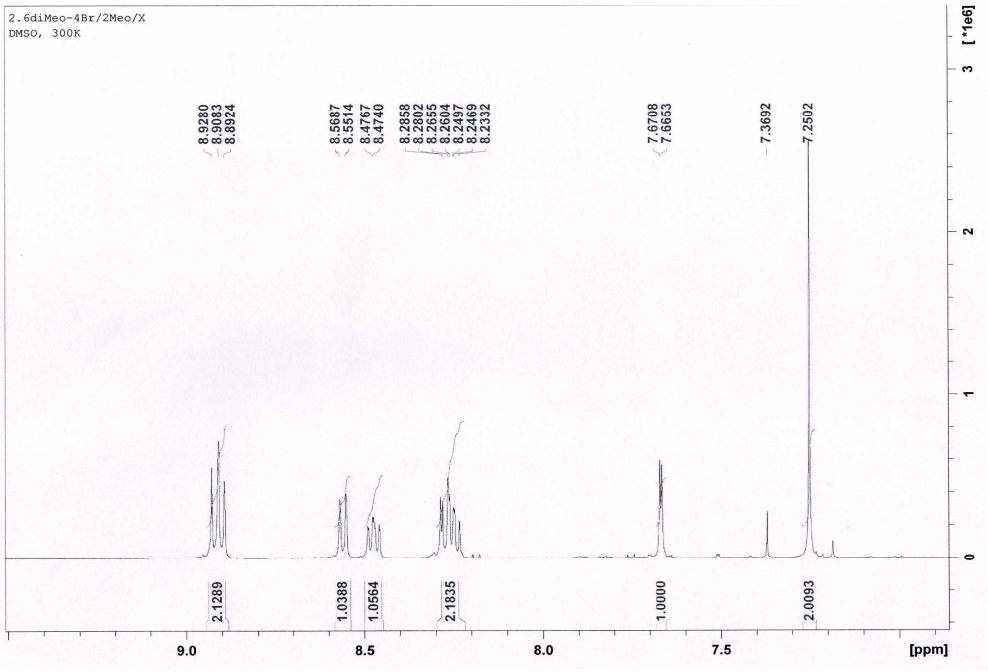

6

aliphatic region

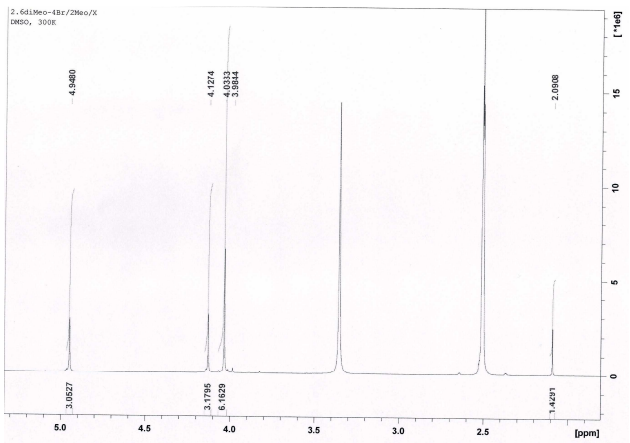

7

aromatic

region

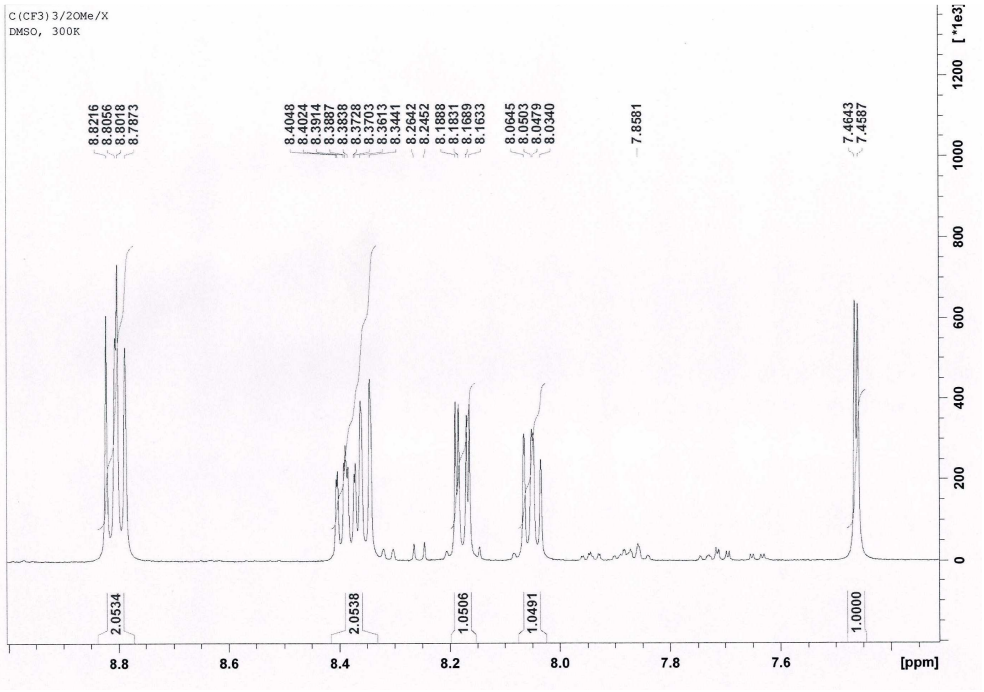

7

aliphatic

region

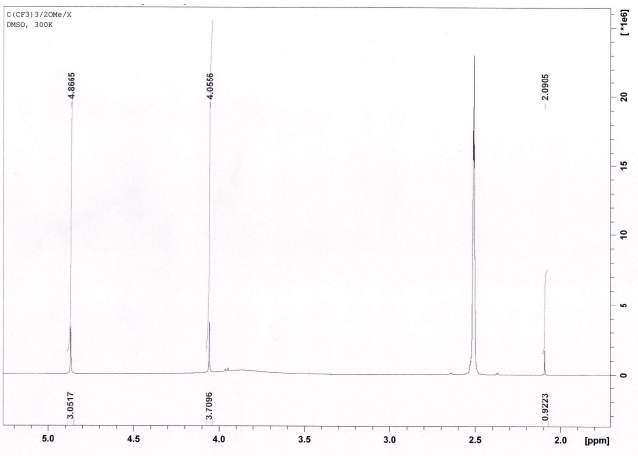

8

aromatic

region

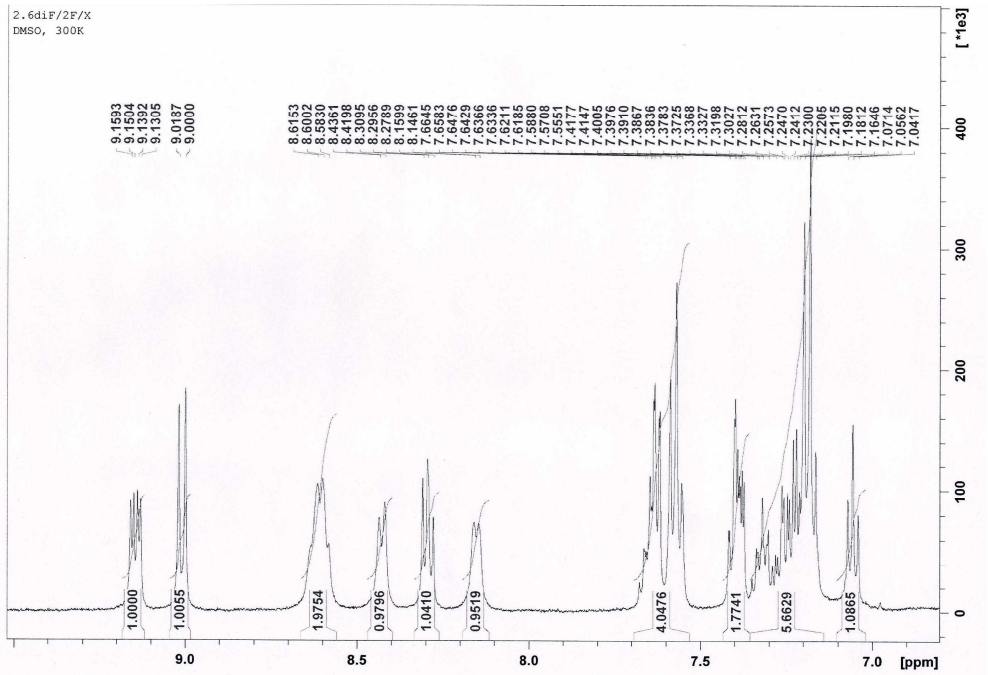

8

aliphatic

region

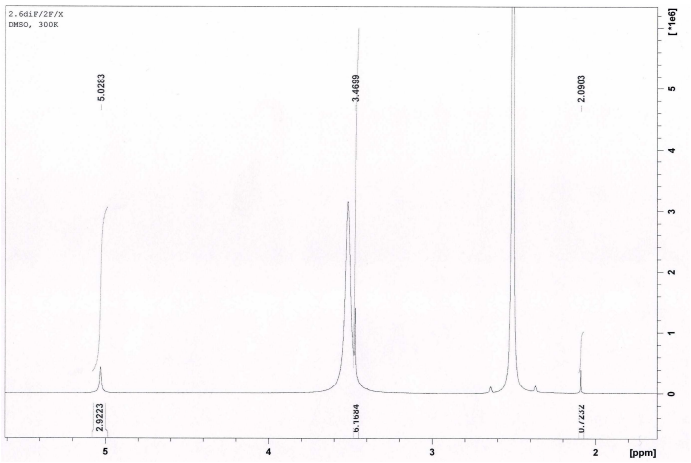

9

aromatic

region

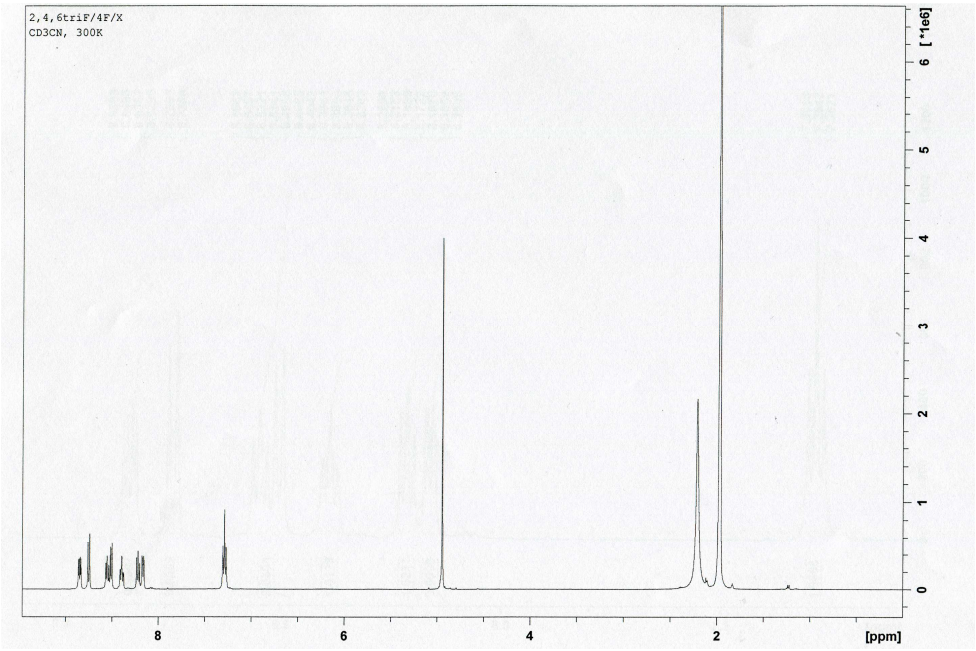

Fig. S4. ^{1}H NMR spectra of compounds **1**−**9** (CMADs, Table 1). Conditions: 500 MHz, DMSO-d6, CD_3CN, T = 298–300 K. For details see the Experimental section.

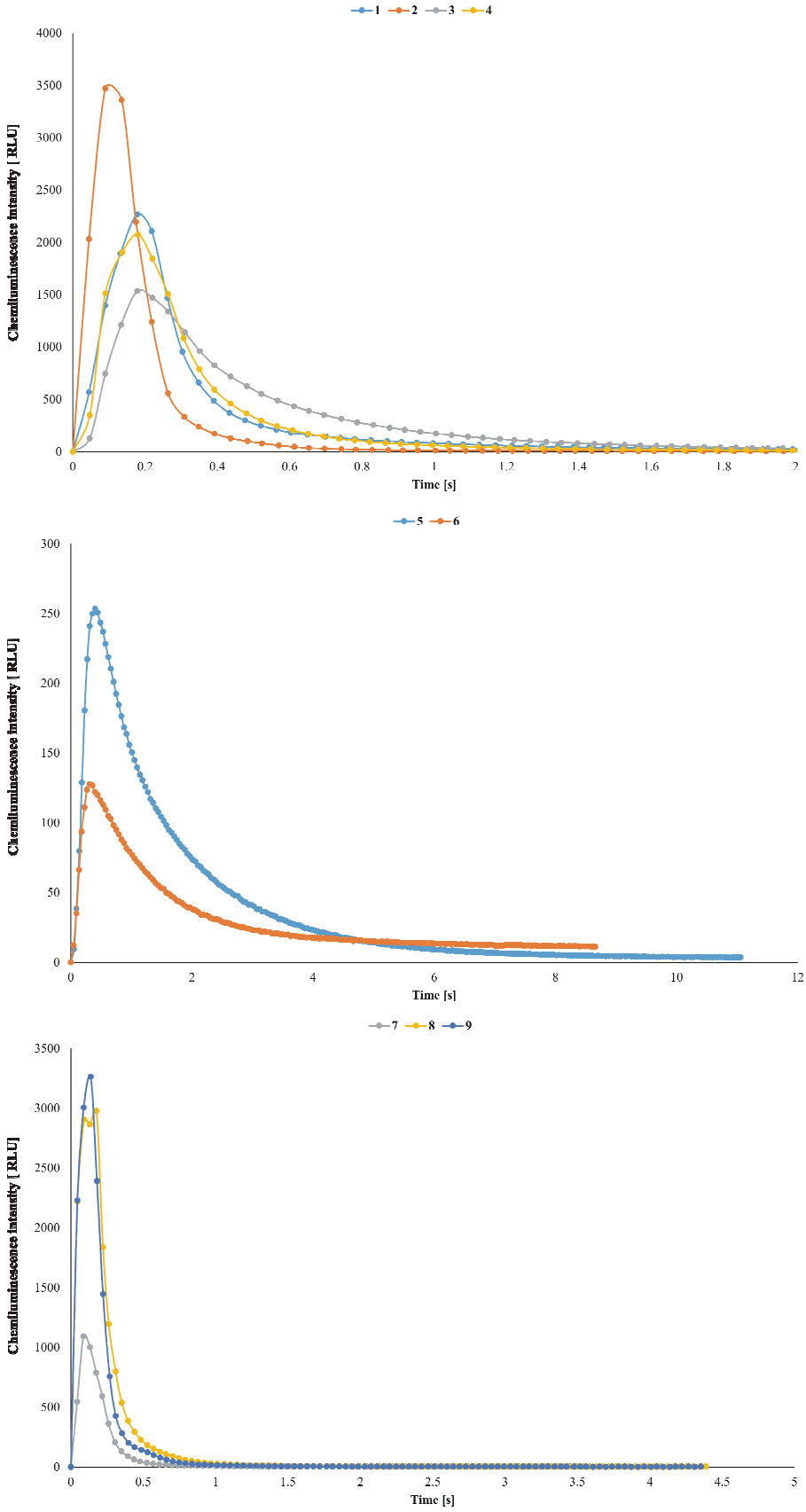

Fig. S5. Time-dependent chemiluminescence intensity, in relative light units (RLU) of CMADs (c(CMAD) = 2×10^{-9} M), triggered in aqueous environment by 0.06 % solution of H_2O_2 in 0.01 M HNO_3 followed 0.2 M NaOH. For details see the Experimental section.

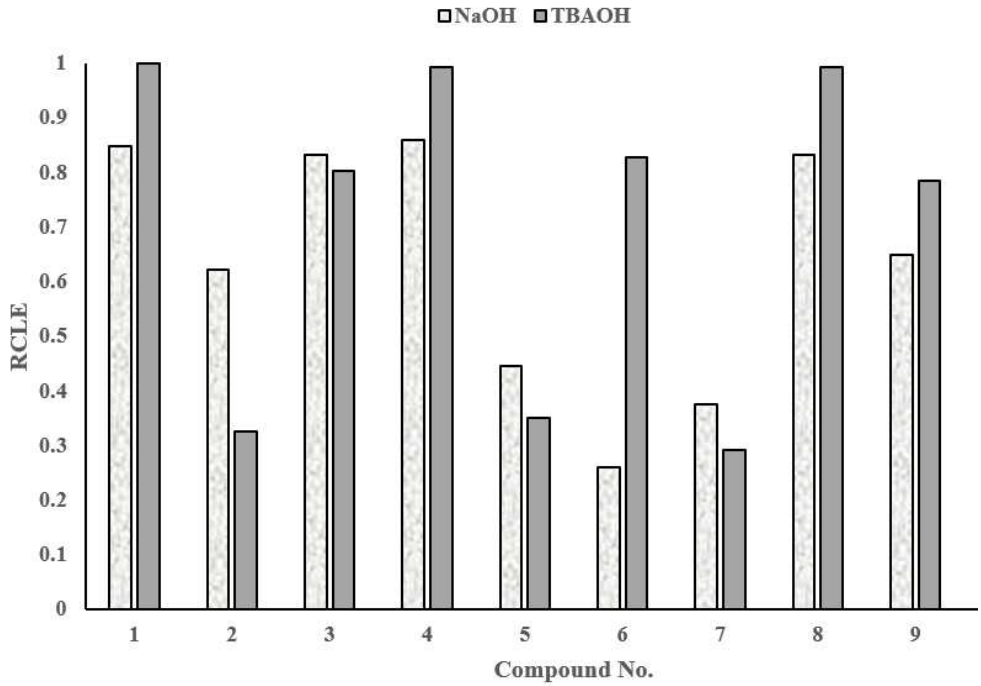

Fig. S6. The relative chemiluminescence efficiencies of CMADs (RCLE; integral emissions, normalized to the highest value in the data set), measured in aqueous environments with the participation of various triggering reagents: 0.06% H_2O_2/0.2 M NaOH and 0.06% H_2O_2/0.2 M TBAOH. For details see the Experimental section.

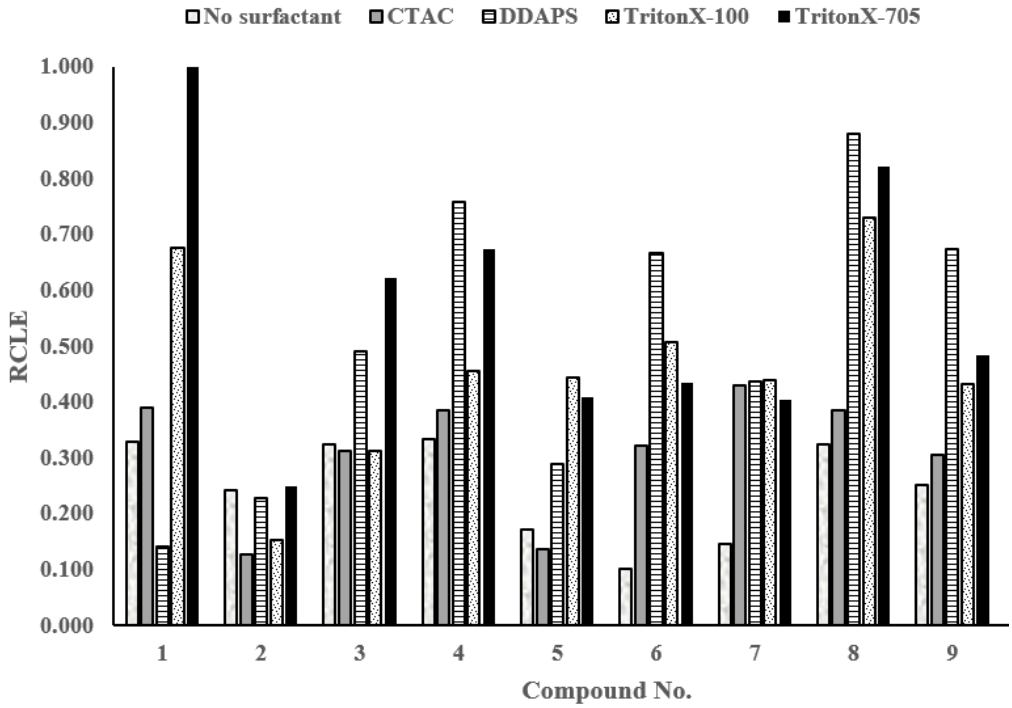

Fig. S7. The changes in relative emission efficiency of CMADs (RCLE; integral values normalized to the highest value in the data set), triggered in aqueous environments by 0.06% solution of H_2O_2 in 0.01 M HNO_3 followed 0.2 M NaOH in the presence of surfactants: cationic (CTAC), zwitterionic (DDAPS) and non-ionic ones (Triton X-100, Triton X-705). For details see the Experimental section.

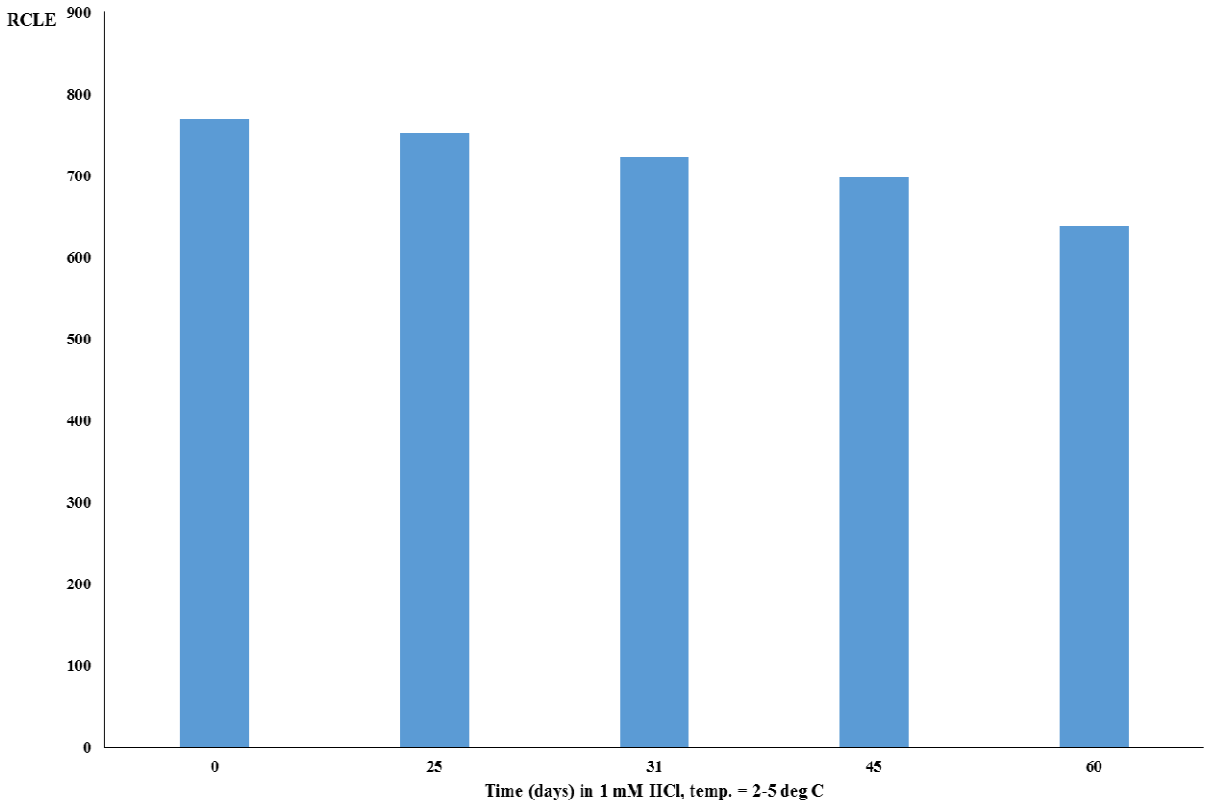

Fig. S8. Long-term storage hydrolytic stability of compound **8** assessed in aqueous acidic conditions (10^{-3} M HCl, 2–5°C).

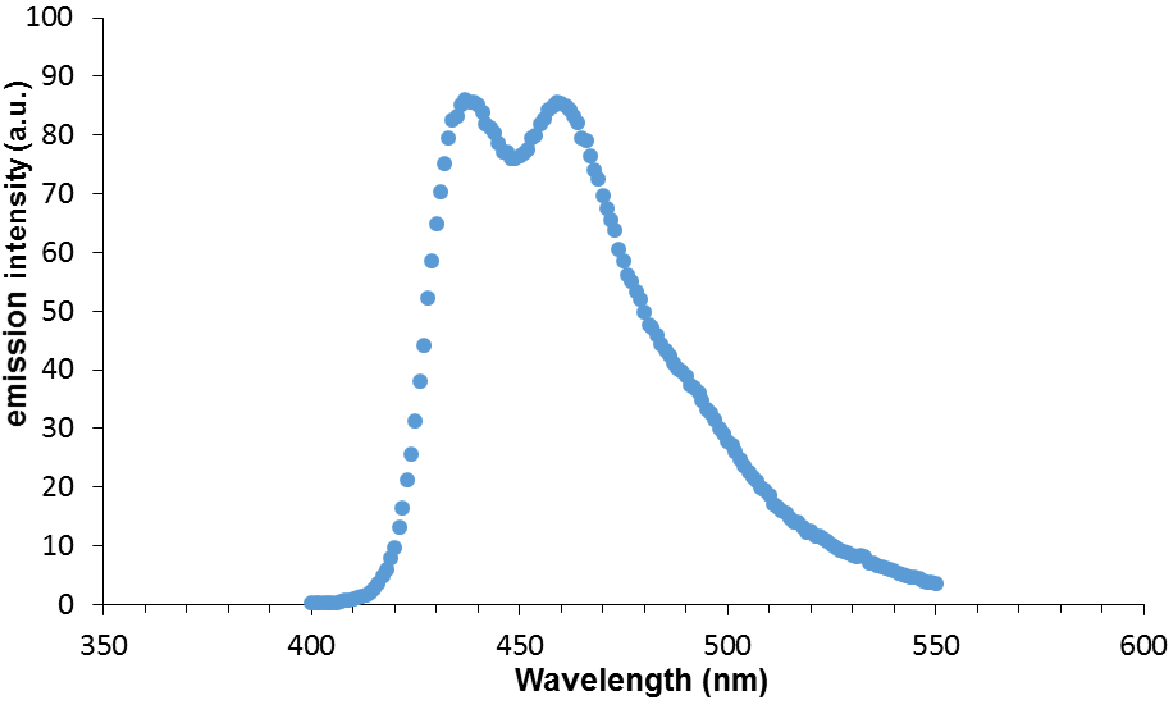

Fig. S9. Stationary chemiluminescence spectra of 2-fluoro-substitued acridnium salts in the acridine ring system (compounds **8**, **9**, Table 1). Experimental details: c(CMAD) = 4×10^{-5} M in 1 mM HCl, triggered in aqueous environments by 0.06% solution of H_2O_2 in 0.01 M HNO_3 followed 0.2 M NaOH in a volume ratio of 2/1/1.

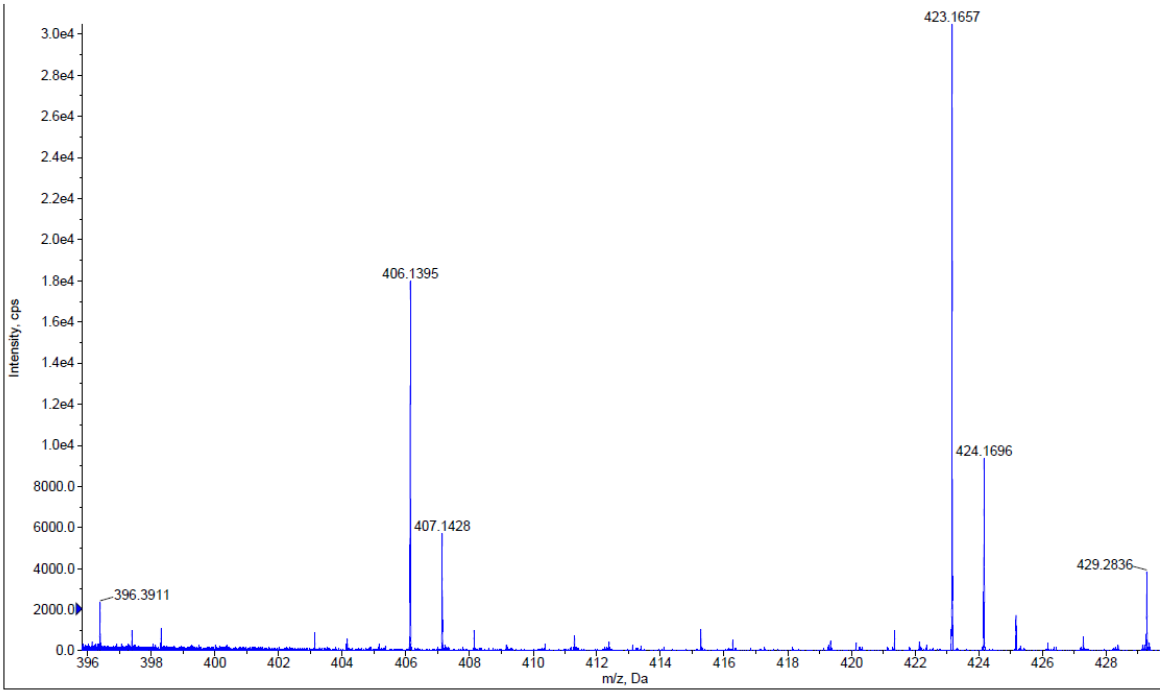

Fig. S10. The signals of hydroxy- and hydroperoxy- radical cationic adducts (CMAD(OH)$^{\bullet+}$, m/z ca. 406) and CMAD(OOH)$^{\bullet+}$, m/z ca. 423) formed with the participation of compound **3** (Table 1) in the presence of $NH_3 \times H_2O/H_2O_2$ mixture under flow-injection conditions of ESI-QTOF MS experiment (see also Table 3 and Fig. 2). For details see the Experimental section.

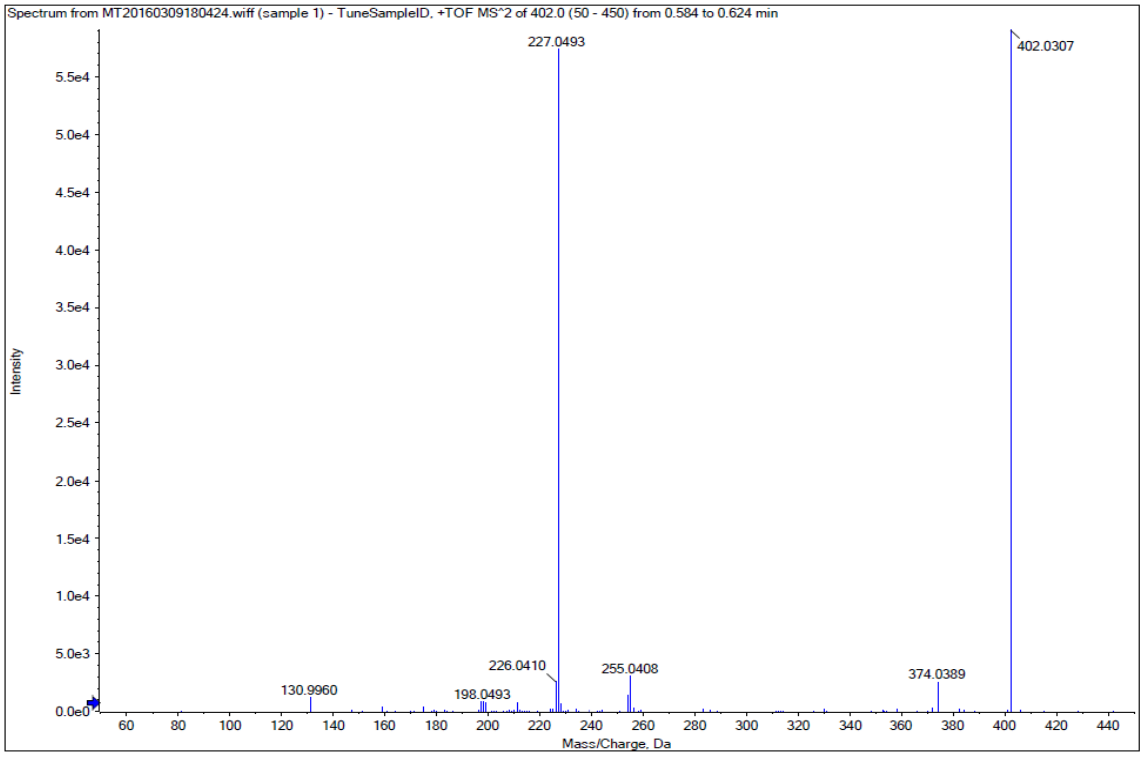

Fig. S11. The ESI-QTOF MS/MS fragmentation of CMAD(OH)$^{\bullet+}$ hydroxy adduct formed with the participation of **9** (m/z = 402.0307) under flow-injection conditions (see also Table 3). For details see the

Experimental section.

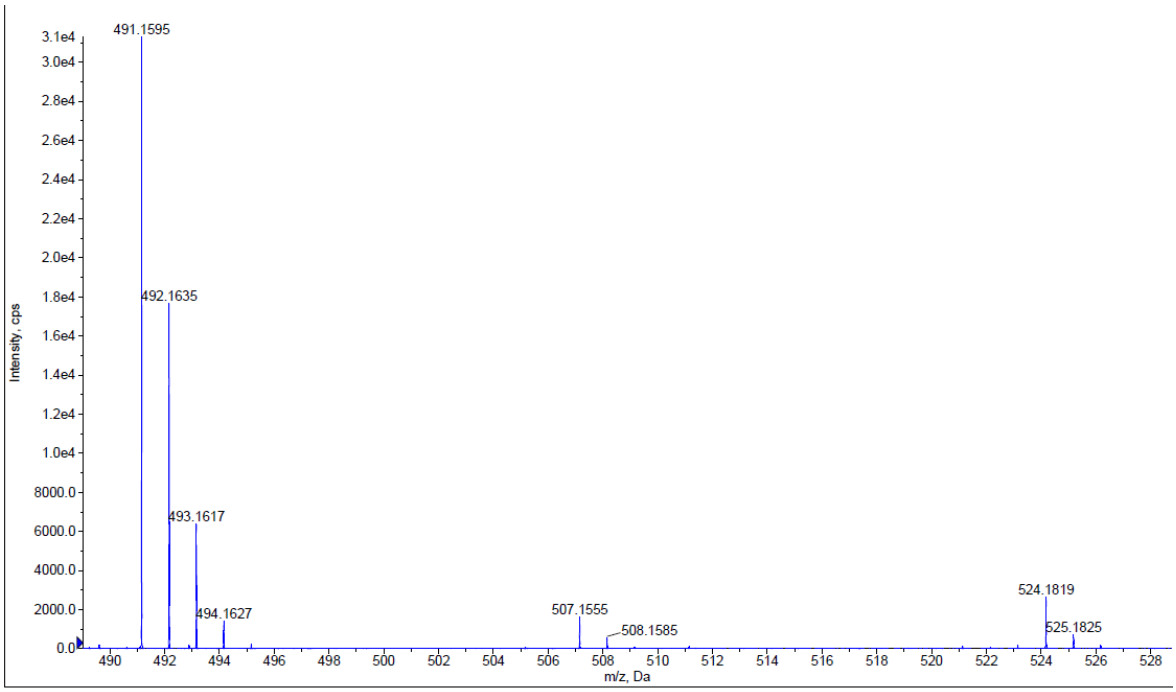

Fig. S12. The signals of hydroxy- and hydroperoxy- radical cationic adducts (CMAD(OH)$^{\bullet+}$ and CMAD(OOH)$^{\bullet+}$, respectively) formed with the participation of compound **5** (Table 1) in the presence of $NH_3 \times H_2O/H_2O_2$ mixture under flow-injection conditions of ESI-QTOF MS experiment (see also Table 3 and Fig. 2). For details see the Experimental section.

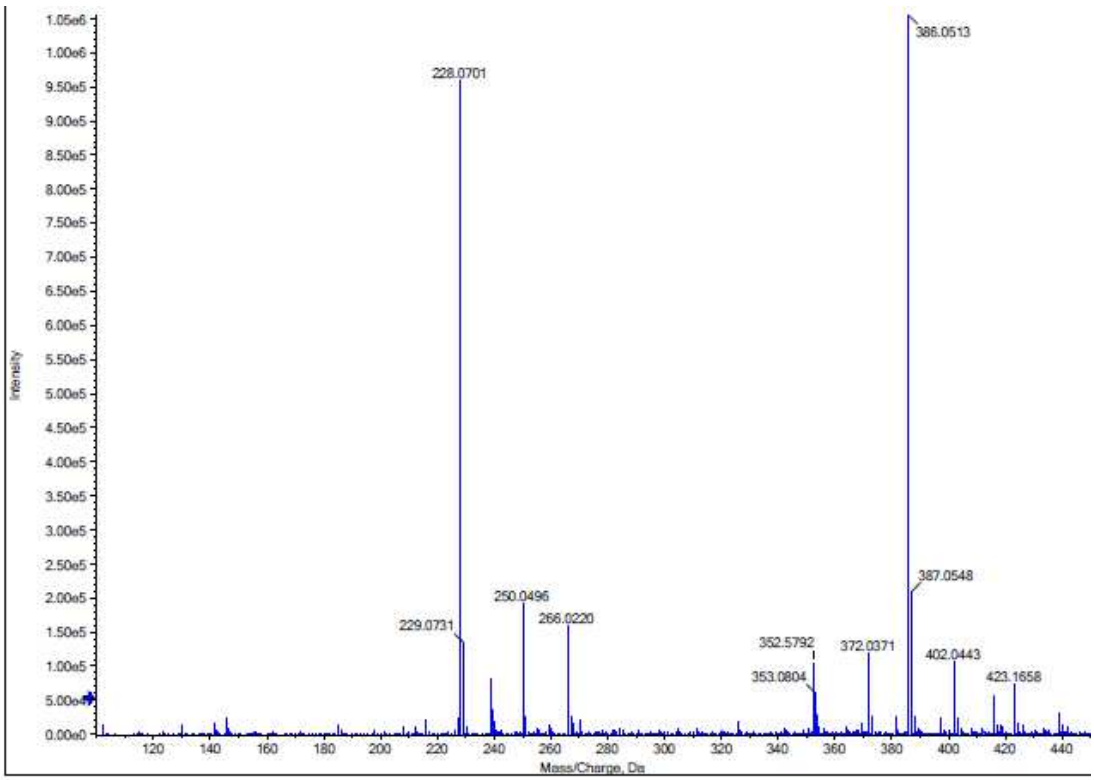

Fig. S13. ESI-QTOF MS spectrum of the post CL reaction mixture (30 sec. after triggering of CL) with the participation of compound **9** (Table 1) in $NH_3 \times H_2O/H_2O_2$ environment. For details see the Experimental section.

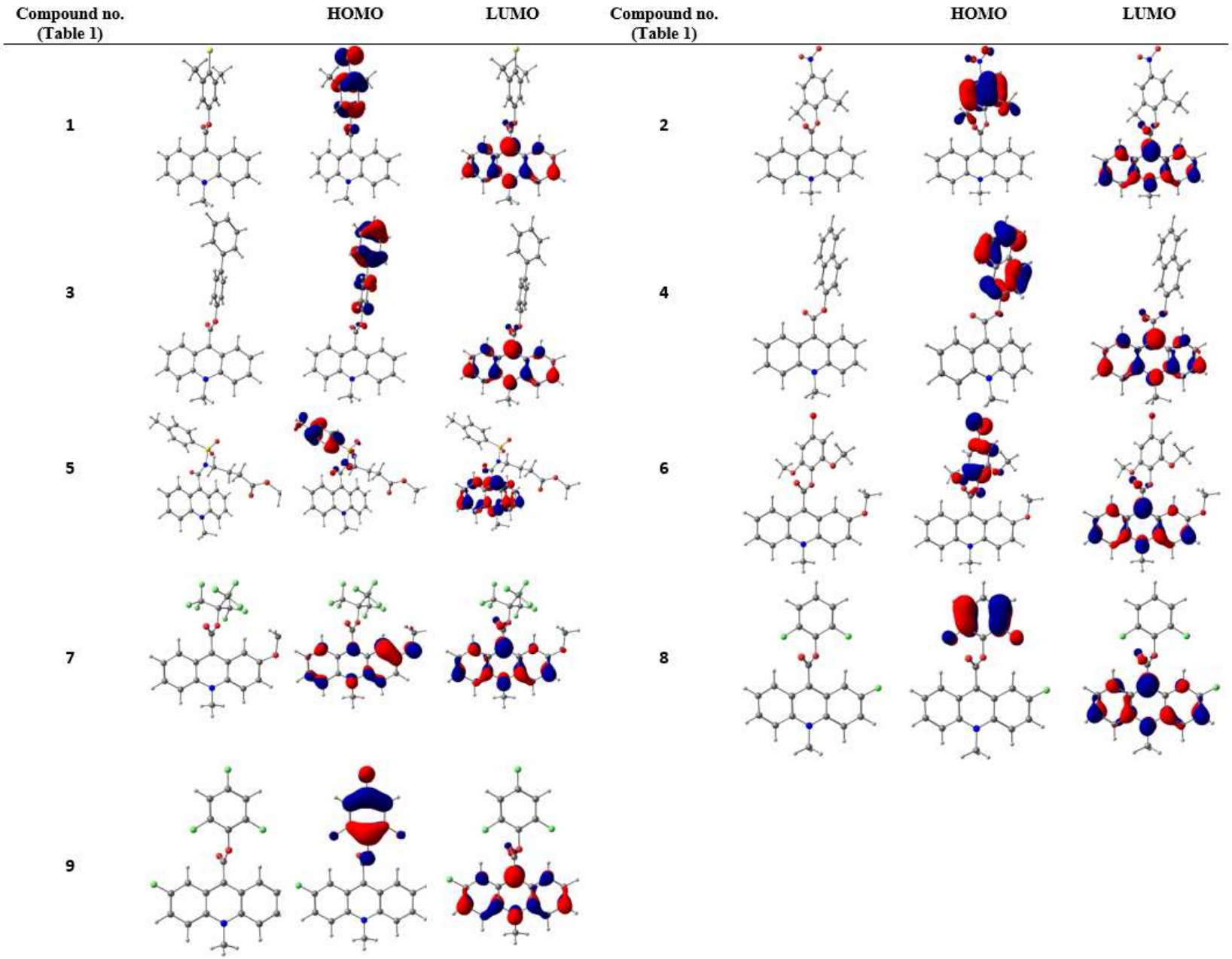

Fig. S14. Computationally predicted structures of investigated compounds (Table 1) and their Highest Occupied (HOMO) and Lowest Unoccupied Molecular Orbitals (LUMO).